TABLE 1

Antiviral activity and enzyme inhibition of protease dimerization inhibitors

MT-2 cells (2×10^3) were exposed to 100 50% tissue culture infectious dose values of HIV-1_{LAI} and cultured in the presence of various concentrations of each drug, and the IC_{50} values were determined using the 3-(4,5-dimethylthiazol-2-yl)-2,5-diphenyltetrazolium bromide assay. All assays were conducted in duplicate, and the data shown represent mean values (±1 S.D.) derived from the results of three independent experiments. The chromogenic substrate Lys-Ala-Arg-Val-Nle-pnitroPhe-Glu-Ala-Nle-amide was used to determine the kinetic parameters. The K_i values were obtained from the IC_{50} values estimated from an inhibitor dose-response curve with the spectroscopic assay using the equation $K_i = (IC_{50} - [E]/2)/(1 + [S]/K_m)$, where $[E]$ and $[S]$ are the PR and substrate concentrations, respectively. The K_i values were measured at four to five substrate concentrations. The measurement was repeated at least three times to produce the average values.

Drug	IC_{50}	K_i
	μM	pM
GRL-0036A	0.005 ± 0.002	29
GRL-06579A	0.0014 ± 0.0008	3.5
GRL-98065	0.0004 ± 0.0001	14
TMC126	0.0003 ± 0.0001	10
DRV	0.0034 ± 0.0005	16
BCV	0.0002 ± 0.0001	6.8
GRL-0026A	0.48 ± 0.04	ND[a]
TPV	0.10 ± 0.04	ND

[a] ND, not determined.

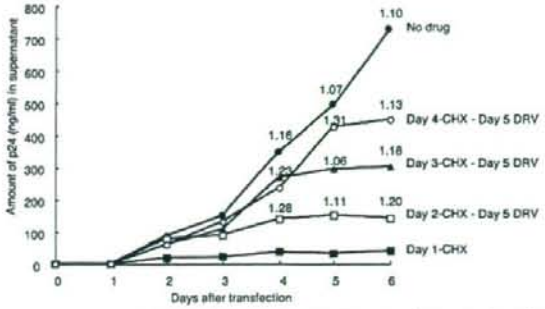

FIGURE 5. **Darunavir does not dissociate once-dimerized protease in cells producing infectious HIV-1 virions.** COS7 cells were co-transfected with two plasmids, pPR_{WT}^{CFP} and pPR_{WT}^{YFP}, exposed to CHX (50 μg/ml) in 24, 48, 72, and 96 h of culture. The cells were exposed to DRV on day 5 of culture. The production of HIV-1 was monitored every 24 h by determining levels of p24 Gag protein produced into culture medium. The values of the $CFP^{A/B}$ ratio were determined at various time points.

administered with ritonavir (38), also blocked protease dimerization (Fig. 4*E*).

We also examined various nucleoside and non-nucleoside reverse transcriptase inhibitors (zidovudine, lamivudine, abacavir, nevirapine, and efavirenz) as well as CCR5 inhibitor aplaviroc (39) for dimerization inhibition. However, none of these anti-HIV-1 agents showed inhibition of dimerization even at relatively higher concentrations of 1–10 μM. Soluble CD4 (5 μg/ml) also failed to inhibit protease dimerization (Fig. 4*G*).

Darunavir Blocks Protease Dimerization as Examined in Dual Luciferase Assay—We also established a dual luciferase assay using the CheckMate™ Mammalian Two-Hybrid System to examine whether DRV blocked protease dimerization in a different assay system. We generated pACT-PR_{WT}, producing PR_{WT}, whose N terminus is connected to the herpes simplex virus VP16 activation domain, and pBIND-PR_{WT}, producing PR_{WT}, whose N terminus is connected to GAL4 DNA-binding domain. In this system, interactions between two different PR_{WT} result in an increase in firefly luciferase expression produced by the pG5*luc* vector. In addition, the pBIND vector expresses *Renilla* luciferase under the control of the SV40 promoter, allowing the user to normalize for the differences in transfection efficiency. Thus, when VP16 and GAL4 closely interact upon protease dimerization, the ratio of the intensity of Fluc over that of Rluc increases, and its decrease indicates the disruption of protease dimerization. As shown in Fig. 4*H*, in the presence of 0.1 and 1 μM of DRV, the relative response ratios significantly decreased, further corroborating that DRV blocks protease dimerization.

Darunavir Does Not Dissociate Once-dimerized Protease in Cells Producing Infectious HIV-1 Virions—Finally, an attempt was made to determine if dimerization inhibitors could dissociate mature protease that had already dimerized. COS7 cells were co-transfected with a pair of plasmids encoding HIV-PR_{WT}^{CFP} and HIV-PR_{WT}^{YFP} and exposed to a protein synthesis inhibitor CHX (50 μg/ml) at 24, 48, 72, and 96 h of culture. The cells were then exposed to DRV on day 5 of culture, the production of HIV-1 was monitored every 24 h by determining levels of p24 Gag protein produced into culture medium, and the values of the $CFP^{A/B}$ ratio were determined at various time points (Fig. 5). When the cells were treated with CHX on day 1 and throughout the rest of the culture period, only a small amount of p24 Gag protein production was seen but no cells emitting fluorescence were observed. When the cells were exposed to CHX on day 2 and beyond, Gag protein production was readily

FIGURE 4. **Inhibition of protease dimerization.** *A*, inhibition of protease dimerization by non-peptidyl and peptidyl compounds. COS7 cells were exposed to each of the agents (1 μM of GRL-0036A, GRL-06579A, GRL-98065, TMC126, DRV, and BCV and 10 μM of P9 and P27) and subsequently co-transfected with pPR_{WT}^{CFP} and pPR_{WT}^{YFP}. After 72 h, cultured cells were examined in the FRET-HIV-1 assay system using confocal microscopy Fluoview FV500 confocal laser scanning microscope, and $CFP^{A/B}$ ratios were determined and plotted. The mean of these ratios obtained are shown as *bars*. *B*, distribution of the values of $CFP^{A/B}$ ratio in the presence of 1 μM DRV. 143 cells obtained from 11 independent assays were examined, and $CFP^{A/B}$ ratios determined were plotted. All the assays were conducted in a blinded manner. *C*, dose-responsive dimerization inhibition by DRV. COS7 cells were exposed to various concentrations of DRV, co-transfected with pPR_{WT}^{CFP} and pPR_{WT}^{YFP}, and A/B ratios were determined. *D*, dose-responsive dimerization inhibition by various non-peptidyl compounds. COS7 cells were exposed to various concentrations of GRL-0026A, TMC126, and BCV, co-transfected with pPR_{WT}^{CFP} and pPR_{WT}^{YFP}, and cultured for 72 h. At the end of the culture, $CFP^{A/B}$ ratio values were determined. *E*, failure of seven clinically available protease inhibitors except DRV and TPV to inhibit the dimerization of PR_{WT}^{CFP} and PR_{WT}^{YFP}. COS7 cells were co-transfected with pPR_{WT}^{CFP} and pPR_{WT}^{YFP} in the presence of various anti-HIV-1 protease inhibitors at concentration of 1 μM, and A/B ratios were determined. *F*, failure of a high concentration of four clinically available protease inhibitors to inhibit HIV-1 protease dimerization. COS7 cells were co-transfected with pPR_{WT}^{CFP} and pPR_{WT}^{YFP} in the presence of four PIs (saquinavir, amprenavir, nelfinavir, and atazanavir) at a higher concentration of 10 μM, cultured for 72 h, and $CFP^{A/B}$ ratios were determined. Note that all the $CFP^{A/B}$ ratio values were >1.0 except for those of DRV. *G*, various approved anti-HIV-1 agents failed to inhibit HIV-1 protease dimerization. COS7 cells were co-transfected with pPR_{WT}^{CFP} and pPR_{WT}^{YFP}. In the presence of various nucleoside and non-nucleoside reverse transcriptase inhibitors (zidovudine, lamivudine, abacavir, nevirapine, and efavirenz), CCR5 inhibitor aplaviroc, and soluble CD4, and A/B ratios were determined. *H*, protease dimerization inhibition by DRV on dual luciferase assay. COS7 cells were co-transfected with pACT-PR_{WT}, pBIND-PR_{WT}, and pG5*luc* in the presence or absence of 0.1 or 1.0 μM of DRV, cultured for 48 h, and the intensity of firefly luminescence (*Fluc*) and *Renilla* luminescence (*Rluc*) was measured with TR717 microplate luminometer. DRV was added to the culture medium simultaneously with plasmids to be used. Fluc/Rluc intensity ratios were determined with co-transfection of pACT-PR_{WT}, pBIND-PR_{WT}, and pG5*luc* in the absence of DRV, serving as maximal values.

detected by day 2, but no significant increment in the production of p24 Gag protein was seen on those days subsequent to the addition of CHX. When the cells were exposed to CHX on days 3 and 4, greater amounts of Gag protein were seen (Fig. 5). The $CFP^{A/B}$ ratios determined on days 4 and 5 of culture were all >1.0, signifying that HIV-1 protease had been generated and dimerization had occurred. On day 5, DRV (1 μM) was added to all the cultures described above and the $CFP^{A/B}$ ratios were determined on day 6 of culture. The ratios remained >1.0 in all of the cultured COS7 cells (Fig. 5). These data strongly suggest that DRV does not dissociate mature protease once dimerized within the HIV-1-producing COS7 cells.

DISCUSSION

In the present study, we developed an intermolecular FRET-based HIV-1-expression assay (FRET-HIV-1 expression assay) that employed cyan and yellow fluorescent protein-tagged HIV-1 protease monomers. Using this assay, we identified a group of non-peptidyl small molecule inhibitors of HIV-1 protease dimerization (molecular weight, 547–704). Dimerization of HIV-1 protease subunits is an essential process for the acquisition of proteolytic activity of HIV-1 protease, which plays a critical role in the replication cycle of HIV-1. Hence, the inhibition of dimerization of HIV-1 protease subunits represents a unique target for potential intervention of HIV-1 replication. The strategy to target protease dimerization as a possible anti-HIV-1 modality has been explored (8, 11–13), and certain compounds have been reported as potential protease dimerization inhibitors. However, no direct evidence of dimerization inhibition by such compounds has been documented. The present report represents the first demonstration that non-peptidic small molecule agents can disrupt protease dimerization.

The structural feature that is in common to the four dimerization inhibitors (TMC126 (33), GRL-98065 (36), DRV (24), and BCV (37)) is that all of these agents contain the structure-based designed privileged cyclic ether-derived non-peptidyl P2 ligand, 3(*R*),3α(*S*),6α(*R*)-bistetrahydrofuranylurethane (bis-THF) and a sulfonamide isostere (22, 23). GRL-0036A and GRL-06579A (26) have bis-THF-related ligand instead of bis-THF. Crystallographic data of dimerized protease complexed with three dimerization inhibitors (GRL-98065 (36), TMC126,[3] and DRV (40)) have revealed that bis-THF forms three tight hydrogen bond interactions with Asp-29 and Asp-30, two highly conserved catalytic site amino acids. We also observed that TPV has the ability to disrupt protease dimerization. TPV, which does not possess the bis-THF component, also has interactions with both Asp-29 and Asp-30 through its pyridinesulfonamide group, as shown in crystallographic analysis of a dimerized protease complexed with TPV (41). Thus, the inhibition of protease dimerization is not inherent only to the bis-THF component.

Most of the dimerization inhibitors we examined in this study exerted potent activity against PI-resistant protease in addition to their potent activity to wild-type HIV-1. DRV is potent against $HIV\text{-}1_{NL4\text{-}3}$ variants exposed to and selected for resistance to saquinavir, indinavir, nelfinavir, and ritonavir (24). Crystal structures of HIV-1 protease with a single mutation (D30N, I50V, V82A, I84V, or L90M) complexed with DRV demonstrate that DRV not only binds to the same catalytic active site as it does for wild-type protease but also maintains hydrogen bond interactions with the backbone atoms of Asp-29 and Asp-30 (40, 42). GRL-06579A and GRL-98065 are also potent against multidrug resistant HIV-1 strains, and molecular modeling indicates that for multidrug-resistant clinical isolates, these inhibitors maintain many of the interactions to critical active site residues (26, 36). TPV, which is active against HIV-1 carrying multidrug-resistant protease, also maintains critical hydrogen bond interactions with backbone atoms in the catalytic active site of mutant protease (43).

It is of note that the D30N-carrying HIV-1 variant is infectious and replication-competent (34). Structural studies do not show any hydrogen bond interactions between two monomer proteases mediated through Asp-30, and the FRET-HIV-1 expression assay showed that D30N mutant did not disrupt protease dimerization. This suggests that Asp-30 is not a critical residue for disrupting protease dimerization, and the interaction of these inhibitors with Asp-30 is not linked to the observed dimerization inhibition. However, potential interactions of dimerization inhibitors such as DRV involving Asp-29 could be critical, because D29N and D29A mutations disrupted protease dimer formation (Fig. 2*E*). Our analysis using the FRET-HIV-1 expression assay also revealed that the introduction of T26A and R87K to HIV-1 protease disrupted protease dimerization (the average $CFP^{A/B}$ ratios were all <1.0 (Fig. 2*E*)). If the protease monomer takes a configuration comparable to that in the dimerized protease, it is possible that the hydrogen bonding of the inhibitors with Asp-29, and/or Thr-26 and Arg-87, both of which are in the vicinity of Asp-29 and could be critical for dimerization, could be associated with the disruption of dimerization process through affecting the intermolecular and/or intramolecular hydrogen bond network (Fig. 2, *B–D*). In this regard, Ishima *et al.* (30) have shown that a truncated protease monomer takes a configuration similar to the one in the mature dimerized protease; however, it is unknown whether the untruncated monomer subunit takes a similar mature configuration. Furthermore, it is not known as to what stage of protease maturation (before dimerization) the dimerization inhibitors reported here bind to the monomer subunit in.

Another possible mechanism of the dimerization inhibition by the agents reported here is that they might interact with another dimerization interface formed by an interdigitation of the N- and C-terminal portions of each monomer (residues 1–5 and 95–99 (Fig. 2*A*)). In this regard, when we introduced a Pro-1 to Ala substitution (P1A), Q2A, I3A, T4A, L5A, T96A, L97A, N98A, or F99A into the replication-competent $HIV\text{-}1_{NL4\text{-}3}$, five substitutions (I3A, L5A, T96A, L97A, and F99A) produced the ratios of less than 1.0, strongly suggesting that most of the protease monomer subunit failed to dimerize with each of these five substitutions. These data confirmed the five amino acids at the N terminus and those at the C terminus are critical for protease dimerization (30–32). There are no polar interactions involving Q2A or T4A, so it is not surprising that

[3] Y. Koh, S. Matsumi, D. Das, M. Amano, D. A. Davis, J. Li, S. Leschenko, A. Baldridge, T. Shioda, R. Yarchoan, A. K. Ghosh, and H. Mitsuya, unpublished observation.

these mutations did not affect dimer formation. However, the failure of P1A and N98A to disrupt dimerization does not necessarily indicate that these amino acids are not critical for protease dimerization. It is possible that conversion to a residue other than alanine may disrupt dimerization.

In the present study, DRV failed to dissociate mature protease dimer (Fig. 5). It is of note that mature dimerized protease has as many as 12 hydrogen bonds in the N- and C-terminal regions, which may explain in part why DRV failed to dissociate two subunits of mature protease. These data also suggest that protease dimerization is inhibited before the association of two protease subunits occurs, probably when protease is in the form of nascent Gag-Pol polyprotein. However, the absence of structural data of nascent forms of protease subunit-containing polyprotein makes it difficult to conclusively predict how the dimerization inhibitors inhibit protease dimerization.

It is noteworthy that the D25N substitution, which is known to render HIV-1 protease enzymatically inactive (44), failed to disrupt dimerization (Fig. 2*E*), showing that catalytically inactive subunits are still capable of undergoing dimerization. This observation indicates that the dimerization inhibition is a differing event than the process that confers catalytic activity on two protease monomer subunits.

DRV has a potent activity against a wide spectrum of HIV-1 isolates, including highly multiprotease-inhibitor-resistant HIV-1 variants. The emergence of DRV-resistant HIV-1 seems to be substantially delayed both *in vitro* (45) and clinical settings (46, 47). One can speculate that DRV inhibits protease dimerization, leaving catalytically inert monomers, but if certain monomers escape from DRV and achieve the mature dimer form, DRV again blocks the proteolytic action of mature (wild-type and mutant) protease as a conventional protease inhibitor. This dual anti-HIV-1 function of DRV may explain why DRV is such a highly effective anti-HIV-1 therapeutic and differentiates it from many of the currently available protease inhibitors (46, 47). It is of note that the plasma concentrations of DRV achieved in those receiving DRV and ritonavir remain >2 μg/ml or ~3.66 μM (48). These concentrations substantially exceed the concentration of DRV effectively disrupting protease dimerization (0.1 μM in culture as shown in Fig. 4*C*). Hence, the dimerization inhibition by DRV should be in operation in the clinical settings. Furthermore, DRV could more efficiently disrupt protease dimerization in individuals with HIV-1 infection receiving DRV and ritonavir, because the protease expression levels upon transfection in this study appear to be considerably greater than the protease expression levels *in vivo*, considering that the p24 production levels could be as high as 500–1500 ng/ml by 5 days following transfection of COS7 cells with plasmids used in the FRET-HIV-1 expression assay. The inhibition of HIV-1 protease dimerization by non-peptidyl small molecule agents represents a unique mechanism of HIV-1 intervention, and the dually functional inhibitors reported here might serve as potential candidates as a new class of therapeutic agents for HIV-1 infection and AIDS. The present data should not only help design and examine agents that potentially inhibit HIV-1 protease dimerization but also should give new insights into the process and dynamics of HIV-1 protease dimerization *per se*.

Acknowledgments—We thank Philip Yin and Kenji Maeda for critical reading of the manuscript, Toshikazu Miyakawa for helpful discussion, and Maki Nakayama for technical assistance.

REFERENCES

1. Simon, V., and Ho, D. D. (2003) *Nat. Rev. Microbiol.* **1,** 181–190
2. Carr, A. (2003) *Nat. Rev. Drug Discov.* **2,** 624–634
3. Wlodawer, A., Miller, M., Jaskolski, M., Sathyanarayana, B. K., Baldwin, E., Weber, I. T., Selk, L. M., Clawson, L., Schneider, J., and Kent, S. B. (1989) *Science* **245,** 616–621
4. Kohl, N. E., Emini, E. A., Schleif, W. A., Davis, L. J., Heimbach, J. C., Dixon, R. A., Scolnick, E. M., and Sigal, I. S. (1988) *Proc. Natl. Acad. Sci. U. S. A.* **85,** 4686–4690
5. Lapatto, R., Blundell, T., Hemmings, A., Overington, J., Wilderspin, A., Wood, S., Merson, J. R., Whittle, P. J., Danley, D. E., Geoghegan, K. F., Hawrylik, S. J., Lee, S. E., Scheld, K. G., and Hobart, P. M. (1989) *Nature* **342,** 299–302
6. Spinelli, S., Liu, Q. Z., Alzari, P. M., Hirel, P. H., and Poljak, R. J. (1991) *Biochimie (Paris)* **73,** 1391–1396
7. Strisovsky, K., Tessmer, U., Langner, J., Konvalinka, J., and Krausslich, H. G. (2000) *Protein Sci.* **9,** 1631–1641
8. Levy, Y., Caflisch, A., Onuchic, J. N., and Wolynes, P. G. (2004) *J. Mol. Biol.* **340,** 67–79
9. Levy, Y., and Caflisch, A. (2003) *J. Phys. Chem. B* **107,** 3068–3079
10. Todd, M. J., Semo, N., and Freire, E. (1998) *J. Mol. Biol.* **283,** 475–488
11. Bowman, M. J., Byrne, S., and Chmielewski, J. (2005) *Chem. Biol.* **12,** 439–444
12. Frutos, S., Rodriguez-Mias, R. A., Madurga, S., Collinet, B., Reboud-Ravaux, M., Ludevid, D., and Giralt, E. (2007) *Biopolymers* **88,** 164–173
13. Bannwarth, L., Kessler, A., Pethe, S., Collinet, B., Merabet, N., Boggetto, N., Sicsic, S., Reboud-Ravaux, M., and Ongeri, S. (2006) *J. Med. Chem.* **49,** 4657–4664
14. Davis, D. A., Brown, C. A., Singer, K. E., Wang, V., Kaufman, J., Stahl, S. J., Wingfield, P., Maeda, K., Harada, S., Yoshimura, K., Kosalaraksa, P., Mitsuya, H., and Yarchoan, R. (2006) *Antiviral Res.* **72,** 89–99
15. Hoess, R. H., and Abremski, K. (1984) *Proc. Natl. Acad. Sci. U. S. A.* **81,** 1026–1029
16. Fang, G., Weiser, B., Visosky, A., Moran, T., and Burger, H. (1999) *Nat. Med.* **5,** 239–242
17. Gatanaga, H., Suzuki, Y., Tsang, H., Yoshimura, K., Kavlick, M. F., Nagashima, K., Gorelick, R. J., Mardy, S., Tang, C., Summers, M. F., and Mitsuya, H. (2002) *J. Biol. Chem.* **277,** 5952–5961
18. Sekar, R. B., and Periasamy, A. (2003) *J. Cell Biol.* **160,** 629–633
19. Bastiaens, P. I., Majoul, I. V., Verveer, P. J., Soling, H. D., and Jovin, T. M. (1996) *EMBO J.* **15,** 4246–4253
20. Bastiaens, P. I., and Jovin, T. M. (1996) *Proc. Natl. Acad. Sci. U. S. A.* **93,** 8407–8412
21. Szczesna-Skorupa, E., Mallah, B., and Kemper, B. (2003) *J. Biol. Chem.* **278,** 31269–31276
22. Ghosh, A. K., Pretzer, E., Cho, H., Hussain, K. A., and Duzgunes, N. (2002) *Antiviral. Res.* **54,** 29–36
23. Ghosh, A. K., Leshchenko, S., and Noetzel, M. (2004) *J. Org. Chem.* **69,** 7822–7829
24. Koh, Y., Nakata, H., Maeda, K., Ogata, H., Bilcer, G., Devasamudram, T., Kincaid, J. F., Boross, P., Wang, Y. F., Tie, Y., Volarath, P., Gaddis, L., Harrison, R. W., Weber, I. T., Ghosh, A. K., and Mitsuya, H. (2003) *Antimicrob. Agents Chemother.* **47,** 3123–3129
25. Kovalevsky, A. Y., Liu, F., Leshchenko, S., Ghosh, A. K., Louis, J. M., Harrison, R. W., and Weber, I. T. (2006) *J. Mol. Biol.* **363,** 161–173
26. Ghosh, A. K., Sridhar, P. R., Leshchenko, S., Hussain, A. K., Li, J., Kovalevsky, A. Y., Walters, D. E., Wedekind, J. E., Grum-Tokars, V., Das, D., Koh, Y., Maeda, K., Gatanaga, H., Weber, I. T., and Mitsuya, H. (2006) *J. Med. Chem.* **49,** 5252–5261
27. Maibaum, J., and Rich, D. H. (1988) *J. Med. Chem.* **31,** 625–629
28. Miyawaki, A., Llopis, J., Heim, R., McCaffery, J. M., Adams, J. A., Ikura, M., and Tsien, R. Y. (1997) *Nature* **388,** 882–887

29. Babe, L. M., Rose, J., and Craik, C. S. (1992) *Protein Sci.* **1,** 1244–1253
30. Ishima, R., Torchia, D. A., Lynch, S. M., Gronenborn, A. M., and Louis, J. M. (2003) *J. Biol. Chem.* **278,** 43311–43319
31. Ishima, R., Ghirlando, R., Tozser, J., Gronenborn, A. M., Torchia, D. A., and Louis, J. M. (2001) *J. Biol. Chem.* **276,** 49110–49116
32. Louis, J. M., Ishima, R., Nesheiwat, I., Pannell, L. K., Lynch, S. M., Torchia, D. A., and Gronenborn, A. M. (2003) *J. Biol. Chem.* **278,** 6085–6092
33. Yoshimura, K., Kato, R., Kavlick, M. F., Nguyen, A., Maroun, V., Maeda, K., Hussain, K. A., Ghosh, A. K., Gulnik, S. V., Erickson, J. W., and Mitsuya, H. (2002) *J. Virol.* **76,** 1349–1358
34. Patick, A. K., Mo, H., Markowitz, M., Appelt, K., Wu, B., Musick, L., Kalish, V., Kaldor, S., Reich, S., Ho, D., and Webber, S. (1996) *Antimicrob. Agents Chemother.* **40,** 292–297
35. Konvalinka, J., Litterst, M. A., Welker, R., Kottler, H., Rippmann, F., Heuser, A. M., and Krausslich, H. G. (1995) *J. Virol.* **69,** 7180–7186
36. Amano, M., Koh, Y., Das, D., Li, J., Leschenko, S., Wang, Y. F., Boross, P. I., Weber, I. T., Ghosh, A. K., and Mitsuya, H. (2007) *Antimicrob. Agents Chemother.* **51,** 2143–2155
37. Miller, J. F., Andrews, C. W., Brieger, M., Furfine, E. S., Hale, M. R., Hanlon, M. H., Hazen, R. J., Kaldor, I., McLean, E. W., Reynolds, D., Sammond, D. M., Spaltenstein, A., Tung, R., Turner, E. M., Xu, R. X., and Sherrill, R. G. (2006) *Bioorg. Med. Chem. Lett.* **16,** 1788–1794
38. Hicks, C. B., Cahn, P., Cooper, D. A., Walmsley, S. L., Katlama, C., Clotet, B., Lazzarin, A., Johnson, M. A., Neubacher, D., Mayers, D., and Valdez, H. (2006) *Lancet* **368,** 466–475
39. Maeda, K., Nakata, H., Koh, Y., Miyakawa, T., Ogata, H., Takaoka, Y., Shibayama, S., Sagawa, K., Fukushima, D., Moravek, J., Koyanagi, Y., and Mitsuya, H. (2004) *J. Virol.* **78,** 8654–8662
40. Tie, Y., Boross, P. I., Wang, Y. F., Gaddis, L., Hussain, A. K., Leshchenko, S., Ghosh, A. K., Louis, J. M., Harrison, R. W., and Weber, I. T. (2004) *J. Mol. Biol.* **338,** 341–352
41. Thaisrivongs, S., Skulnick, H. I., Turner, S. R., Strohbach, J. W., Tommasi, R. A., Johnson, P. D., Aristoff, P. A., Judge, T. M., Gammill, R. B., Morris, J. K., Romines, K. R., Chrusciel, R. A., Hinshaw, R. R., Chong, K. T., Tarpley, W. G., Poppe, S. M., Slade, D. E., Lynn, J. C., Horng, M. M., Tomich, P. K., Seest, E. P., Dolak, L. A., Howe, W. J., Howard, G. M., Schwende, F. J., Toth, L. N., Padbury, G. E., Wilson, G. J., Shiou, L., Zipp, G. L., Wilkinson, K. F., Rush, B. D., Ruwart, M. J., Koeplinger, K. A., Zhao, Z., Cole, S., Zaya, R. M., Kakuk, T. J., Janakiraman, M. N., and Watenpaugh, K. D. (1996) *J. Med. Chem.* **39,** 4349–4353
42. Kovalevsky, A. Y., Tie, Y., Liu, F., Boross, P. I., Wang, Y. F., Leshchenko, S., Ghosh, A. K., Harrison, R. W., and Weber, I. T. (2006) *J. Med. Chem.* **49,** 1379–1387
43. Muzammil, S., Armstrong, A. A., Kang, L. W., Jakalian, A., Bonneau, P. R., Schmelmer, V., Amzel, L. M., and Freire, E. (2007) *J. Virol.* **81,** 5144–5154
44. Prabu-Jeyabalan, M., Nalivaika, E. A., Romano, K., and Schiffer, C. A. (2006) *J. Virol.* **80,** 3607–3616
45. De Meyer, S., Azijn, H., Surleraux, D., Jochmans, D., Tahri, A., Pauwels, R., Wigerinck, P., and de Bethune, M. P. (2005) *Antimicrob. Agents Chemother.* **49,** 2314–2321
46. Poveda, E., Blanco, F., Garcia-Gasco, P., Alcolea, A., Briz, V., and Soriano, V. (2006) *AIDS* **20,** 1558–1560
47. Youle, M., Staszweski, S., Clotet, B., Arribas, J. R., Blaxhult, A., Carosi, G., Dejesus, E., Di Perri, G., Estrada, V., Fisher, M., Kovacs, C., Kulasegaram, R., Lazzarin, A., Marriott, D., Munoz, L., Reynes, J., Shalit, P., Slim, J., Tsoukas, C., Vaccaro, A., and Vera, J. (2006) *HIV Clin. Trials* **7,** 86–96
48. Hoetelmans, R., Van der Sandt, I., De Pauw, M., Struble, K., Peeters, M., and Van der Geest, R. (2003) *10th Conference on Retroviruses and Opportunistic Infections*, Boston, February 10–14, 2003, Abstr. 549, Foundation for Retrovirology and Human Health, Alexandria, VA

JOURNAL OF VIROLOGY, Apr. 2007, p. 3757–3768 Vol. 81, No. 8
0022-538X/07/$08.00+0 doi:10.1128/JVI.01544-06

Impact of V2 Mutations on Escape from a Potent Neutralizing Anti-V3 Monoclonal Antibody during In Vitro Selection of a Primary Human Immunodeficiency Virus Type 1 Isolate[▽]

Junji Shibata,[1] Kazuhisa Yoshimura,[1] Akiko Honda,[1] Atsushi Koito,[1] Toshio Murakami,[2] and Shuzo Matsushita[1]*

Division of Clinical Retrovirology and Infectious Diseases, Center for AIDS Research, Kumamoto University, Kumamoto 860-0811,[1] and The Chemo-Sero-Therapeutic Research Institute, Kyokushi, Kikuchi, Kumamoto 869-1298,[2] Japan

Received 19 July 2006/Accepted 16 January 2007

KD-247, a humanized monoclonal antibody to an epitope of gp120-V3 tip, has potent cross-neutralizing activity against subtype B primary human immunodeficiency virus type 1 (HIV-1) isolates. To assess how KD-247 escape mutants can be generated, we induced escape variants by exposing bulked primary R5 virus, MOKW, to increasing concentrations of KD-247 in vitro. In the presence of relatively low concentrations of KD-247, viruses with two amino acid mutations (R166K/D167N) in V2 expanded, and under high KD-247 pressure, a V3 tip substitution (P313L) emerged in addition to the V2 mutations. However, a virus with a V2 175P mutation dominated during passaging in the absence of KD-247. Using domain swapping analysis, we demonstrated that the V2 mutations and the P313L mutation in V3 contribute to partial and complete resistance phenotypes against KD-247, respectively. To identify the V2 mutation responsible for the resistance to KD-247, we constructed pseudoviruses with single or double amino acid mutations in V2 and measured their sensitivity to neutralization. Interestingly, the neutralization phenotypes were switched, so that amino acid residue 175 (Pro or Leu) located in the center of V2 was exchanged, indicating that the amino acid at position 175 has a crucial role, dramatically changing the Env oligomeric state on the membrane surface and affecting the neutralization phenotype against not only anti-V3 antibody but also recombinant soluble CD4. These data suggested that HIV-1 can escape from anti-V3 antibody attack by changing the conformation of the functional envelope oligomer by acquiring mutations in the V2 region in environments with relatively low antibody concentrations.

The envelope protein (Env) of human immunodeficiency virus type 1 (HIV-1) presents on the virus surface as "spikes" composed of trimers comprising three gp120-gp41 complexes (6, 32, 33). Among the regions that induce the neutralization antibody (NAb) response, the third variable domain (V3 loop) of gp120 is considered one of the major targets of the host immune response (23, 69). It has been estimated that as much as half of the antibody response against HIV-1 Env in patient serum is directed against the V3 region (43). A recent crystallographic study revealed that the V3 loop contains features that are essential for coreceptor binding and that the extended nature and antibody accessibility of V3 are associated with its immunodominance (20).

HIV-1 primary isolates are relatively resistant to neutralization by NAbs and recombinant soluble CD4 (rsCD4) compared with variants selected for growth in permanent cell lines (42, 52, 55). Studies addressing differences between neutralization-sensitive and -resistant variants have revealed the involvement of several mechanisms that underlie the neutralization resistance of primary isolates, including the occlusion of epitopes within the oligomer, extensive glycosylation, and extension of variable loops from the surface of the complex, as well as steric and conformational blocking of receptor binding sites (7, 12, 32, 38, 49, 50, 54, 62). The structural features of gp120 tolerate a vast array of mutations that permit the selection of neutralization escape variants, as has been previously demonstrated in culture assays, animal models, and infected individuals (24).

Although there are ample data showing that NAbs can protect against HIV-1 infection in vitro and in animal models in vivo, activity in infected humans remains controversial (3, 4, 9, 14, 22, 40, 48, 58). Studies addressing NAbs in primary infections have suggested that most recently infected individuals mount a vigorous antibody response against autologous viruses. However, the rapid evolution of HIV in the presence of NAbs results in the emergence of escape mutants. As a consequence, at any time during an early stage of the HIV disease, NAbs are more likely to recognize earlier autologous viruses than contemporaneous ones. Despite evidence of phenotypic resistance, the genetic basis of the mechanism allowing primary viruses to escape from NAbs is poorly understood. Wei et al. found that glycosylation in the envelope plays an important role in allowing escape from neutralization (62). In contrast, in a recent study Frost et al. found that viral escape from NAbs is correlated with the rate of amino acid substitution rather than changes in glycosylation or insertions or deletions in the envelope (14). Because of the polyclonal nature of NAbs in patient sera, it is difficult to clarify the genetic mechanism responsible for neutralization escape.

* Corresponding author. Mailing address: Division of Clinical Retrovirology and Infectious Diseases, Center for AIDS Research, Kumamoto University, Kumamoto 860-0811, Japan. Phone: 81 96 373 6536. Fax: 81 96 373 6537. E-mail: shuzo@kaiju.medic.kumamoto-u.ac.jp.

▽ Published ahead of print on 24 January 2007.

Neutralization escape from anti-V3 monoclonal antibodies (MAbs) has been induced in T-cell-line-adapted viruses in several experiments and associated with amino acid substitution within the epitope in the V3 loop (8, 37, 65). However, Park et al. showed that human sera with neutralizing antibodies that contained polyclonal antibodies directed at the V3 region induced neutralization-resistant variants without V3 amino acid substitution (46). Neutralization studies using anti-V3 antibodies against primary isolates suggest that the neutralization resistance phenotype is associated with changes in the sequences outside V3, rather than variation within the V3 epitope (29, 62). However, the contribution of each change in the envelope to the emergence of escape mutants remains unclear because they are not selected under neutralizing MAb pressure.

Recently, we described a humanized MAb, KD-247, that displayed cross-neutralizing activity against HIV-1 clade B isolates (11). The epitope of KD-247 was mapped to six amino acids around the PGR core sequence at the tip of the V3 loop. The shortest reactive peptide recognized by KD-247 was determined to be IGPGR, which is shared by 49% of HIV-1 isolates in clade B (35). In addition, complete protection from challenge infection by a pathogenic strain of simian-human immunodeficiency virus 89.6 was observed when a high concentration of the antibody was used in an animal model (10). A molecularly cloned CCR5-tropic HIV-1 strain, JR-FL, which is relatively resistant to neutralization (15, 50), was exposed to KD-247 to obtain a neutralization escape mutant (67). Induction of the neutralization-resistant virus with a mutation in the V3 tip was observed in the presence of a high concentration of KD-247, and the escape variant was found to be more sensitive to CCR5 inhibitors and rsCD4 than the original strain (67).

The present study sought to understand how virus mutation impacts the activity of an anti-V3 MAb, KD-247. For this we subjected a primary R5 virus, MOKW, to selection pressure by KD-247. The present data suggested that it is necessary to pass a phased step so that the escape mutant against the anti-V3 antibody can emerge. Neutralization escape variants with V2 mutations in gp120 could be selected at relatively low KD-247 pressures, but high concentrations of KD-247 were required for induction of a completely resistant variant with amino acid substitution in the epitope. Moreover, we present evidence suggesting that some V2 mutations change the tertiary or quaternary structure of the envelope trimers on the viral surface that are involved in the neutralization resistance of the primary isolate. Clarification of the mechanisms responsible for this neutralization resistance may provide important insight into possible methods for the induction of potent and cross-neutralizing antibody responses capable of neutralizing various primary isolates.

(This work was presented in part at the 13th Conference on Retroviruses and Opportunistic Infection, Denver, CO, 5 to 8 February 2006 [55a].)

MATERIALS AND METHODS

Cells, culture conditions, reagents, and viruses. PM1/CCR5 cells (68) were maintained in RPMI 1640 medium (Sigma) supplemented with 10% heat-inactivated fetal calf serum (FCS; HyClone Laboratories, Logan, UT), 50 U/ml of penicillin, 50 mg/ml of streptomycin, and 100 μg/ml of G418 (Sigma). 293T cells were maintained in Dulbecco's modified Eagle medium (Sigma) supplemented with 10% heat-inactivated FCS. The CD4- and CCR5-expressing human osteogenic sarcoma cell line GHOST-hi5 was maintained in Dulbecco's modified Eagle medium supplemented with 10% FCS, G418 (200 μg/ml), hygromycin B (100 μg/ml; Sigma), and puromycin (1 μg/ml; Sigma).

KD-247, an anti-gp120-V3 antibody, was produced as previously described (11). 17b, a monoclonal antibody against the CD4-induced epitope, and immunoglobulin Gb12 (IgGb12), a monoclonal antibody against the CD4-binding epitope, were provided by the National Institutes of Health AIDS Research and Reference Reagent Program. 447-52D, an anti-gp120 V3 MAb, was a gift from Suzan Zolla-Pazner (New York University School of Medicine). 2D7, an anti-CCR5 MAb, and RPA-T4, an anti-CD4 MAb, were purchased from BD Biosciences Pharmingen (San Jose, CA). Human rsCD4 was purchased from R&D Systems, Inc. (Minneapolis, MN). TAK-779, a CCR5 inhibitor, was kindly provided by Takeda Chemical Industries, Ltd. (Osaka, Japan). AK-602, a CCR5 inhibitor, was gifted by Ono Pharmaceutical Co., Ltd. (Osaka, Japan).

The R5 primary HIV-1, MOKW virus, was isolated from a drug-naïve Japanese patient (36). This virus was passaged in phytohemagglutinin-activated peripheral blood mononuclear cells (PBMCs), and the culture supernatant was stored at −80°C until use.

Isolation of a KD-247-resistant mutant from MOKW virus in vitro. The selection of KD-247 escape variants from MOKW virus was performed as previously described (67). Briefly, MOKW virus was preincubated in the presence of KD-247 for 30 min at 37°C, and then PM1/CCR5 cells (4×10^4) were exposed to 500 times the 50% tissue culture infective dose ($TCID_{50}$) of the preincubated MOKW. After incubation for 5 h at 37°C, cells were pelleted down and resuspended in RPMI 1640 medium supplemented with 10% FCS without KD-247. Viral replication was monitored by observation of the cytopathic effects in PM1/CCR5 cells. The culture supernatant was harvested on day 7 and used to infect fresh PM1/CCR5 cells for the next round of culture in the presence of increasing concentrations of KD-247. When the virus began to propagate rapidly in the presence of KD-247, the MAb concentration was further increased. After the virus was passaged in the presence of up to 2,000 μg/ml KD-247 in PM1/CCR5 cells, a KD-247-resistant virus, MOKW9p(2000), was recovered from the cell culture supernatant. MOKW virus was also passaged for the same time period in PM1/CCR5 cells in the absence of KD-247, and the resulting virus was designated MOKW9p(−).

Amplification of viral cDNA and nucleotide sequencing. Viral RNA was extracted from cell culture supernatants with several concentrations of KD-247 using a QIAamp viral RNA kit (QIAGEN). Viral RNAs were reverse transcribed using a High Capacity cDNA Archive Kit (Applied Biosystems) with specific antisense primer ENVN (5′-CTGCCAATCAGGGAAGTAGCCTTGT GT-3′). Nested PCR was performed to amplify the gp120 C1 to C4 coding region as described previously (60). The primers used were as follows: for the first-step PCR, 1B (5′-AGAAAGAGCAGAAGACAGTGGCAATGA-3′) and H (5′-TA GTGCTTCCTGCTGCTCCCAAGAACCC-3′); for the second-step PCR, 2B (5′-AGCAGAAGACAGTGGCAATGAGAGTGA-3′) and F (5′-ATATAATT CACTTCTCCAATTGTCCCTCAT-3′). The products of the nested PCR were inserted in the TA vector (Invitrogen) and sequenced using a Big Dye Terminator, version 1.1 (Applied Biosystems), in accordance with the manufacturer's instructions.

MTT assay. The neutralization-sensitivities of each passaged MOKW virus to KD-247 were determined as previously described (67). Briefly, PM1/CCR5 cells (2×10^5 cells/well) were exposed to 100 $TCID_{50}$ of each passaged virus in the presence of various concentrations of KD-247 in 96-well round-bottom microculture plates and incubated at 37°C for 7 days. After removal of 100 μl of medium from each well, 10 μl of MTT (3-[4,5-dimethylthiazol-2-yl]-2,5-diphenyl tetrazolium bromide) solution (7.5 mg/ml) in phosphate-buffered saline (PBS) was added to each well, and the plate was incubated at 37°C for 3 h. After incubation, 100 μl of acidified isopropanol containing 4% (vol/vol) Triton X-100 was added to each well to dissolve the formazan crystals. The optical density (wavelength, 570 nm) was measured using a microplate reader. Assays were performed in duplicate or triplicate.

Construction of mutant envelope expression vectors. Proviral DNA was extracted from each batch of passaged MOKW virus-infected PM1/CCR5 cells using a QIAamp DNA blood mini kit (QIAGEN). For the construction of each passaged envelope expression vector, we used pCXN2, which has a chicken actin promoter. Briefly, we amplified MOKW gp160 regions using LA *Taq* (Takara) with primers ENVA (5′-GGCTTAGGCATCTCCTATGGCAGGAAGAA-3′) and ENVN (see above). The products of the PCR were inserted into pCR-XL-TOPO (Invitrogen). The sequences of the amplified *env* region of MOKW virus were confirmed using an ABI377 automated DNA sequencer. The EcoRI fragment of pCR-XL-MOKW containing the entire *env* region was ligated into pCXN2 to give pCXN-MOKW-RDP (the last three letters of the MOKW virus

constructs represent the amino acids at positions 166, 167, and 175 in the V2 region), pCXN-MOKW-KNL/C3m, and pCXN-MOKW-KNL/V3m. The pCXN-MOKW-KNL vector was constructed by replacing the StuI-Bsu36I fragment of pCXN-MOKW-KNL/C3m with a corresponding MOKW-RDP fragment. The pCXN-MOKW-RDP/V3m and pCXN-MOKW-RDP/C3m vectors were constructed by replacing the StuI-Bsu36I fragment of pCXN-MOKW-RDP with the corresponding pCXN-MOKW-KNL/V3m or pCXN-MOKW-KNL/C3m fragments, respectively. pCXN-MOKW-KNP, pCXN-MOKW-RDL, pCXN-MOKW-KDL, and pCXN-MOKW-RNL were generated by site-directed mutagenesis using a QuickChange Site-Directed Mutagenesis Kit (Stratagene) in accordance with the manufacturer's instructions.

Pseudovirus preparation. Five micrograms of pNL4-3.luc.R$^-$E$^-$ and 0.5 μg of pRSV-Rev (18), supplied by the NIH AIDS Research and Reference Reagent Program, and 4.5 μg of the MOKW Env-expressing pCXN2 were cotransfected into 293T cells using Effectene transfection reagent (QIAGEN). At 24 h after the transfection, the pseudovirus-containing supernatants were harvested, filtered through a 0.2-μm-pore-size filter, and stored at −80°C. To measure the pseudovirus activity, a luminescence assay using GHOST-hi5 cells was used as previously described (60).

Neutralization assays. A single-cycle infectivity assay was used to measure the neutralization of MOKW pseudoviruses as described previously (60). Briefly, MAbs at various concentrations and a pseudovirus suspension corresponding to 100 $TCID_{50}$ were preincubated on ice for 15 min. The virus-antibody mixtures were added to GHOST-hi5 cells, which on the preceding day had been seeded in a 96-well plate (1.5×10^4 cells/well). Cultures were incubated for 2 days at 37°C, washed with PBS, and lysed with lysis buffer (Luc PGC-50; PicaGene). Following transfer of the cell lysates to luminometer plates (Coastar 3912), the luciferase activity (in relative light units) in each well was measured using luciferase substrate (100 μl/well; PicaGene) in a TR717 microplate luminometer (Applied Biosystems). The reduction in infectivity was determined by comparing the relative light units in the presence and absence of MAbs and was expressed as the percentage of neutralization. The same assay was repeated two to three times.

In vitro binding assay to the MOKW envelope-expressing cell surfaces. In vitro binding assays were performed as previously described (53, 67). EcoRI fragments of MOKW *env* genes from pXL-MOKWs were subcloned into the corresponding sites in pDNR-1r (Clontech). The vectors were sequenced to confirm the presence of the desired *env* gene and the absence of other changes. The *env* gene fragments were then subcloned into pLP-IRES2-EGFP (Clontech) using Cre-recombinase (Clontech) in accordance with the manufacturer's instructions. 293T cells were cotransfected with pRSV-Rev (0.5 μg) and pLP-IRES2-EGFP-MOKW (9.5 μg) using the Effectene transfection reagent. After 36 h, the cells were harvested, incubated with each anti-HIV-1 MAb in combination with biotin-conjugated anti-human IgG and peridinin chlorophyll protein-conjugated streptavidin (BD Pharmingen), gated for the green fluorescent protein (GFP)-positive area, and analyzed using a FACSCalibur flow cytometry system.

MAb-gp120 binding assay. Culture supernatants containing the pseudotyped viruses were treated with 1% nonionic Nonidet P-40 to provide a source of gp120. Binding assays for MAbs to gp120 were then performed essentially as described elsewhere (41, 59). Briefly, gp120 proteins from transfected culture supernatants, diluted in Tris-buffered saline containing 10% FCS and 1% Nonidet P-40, were captured onto solid phase via their carboxyl termini using sheep polyclonal antibody D7324 (Aalto Bioreagents, Dublin, Ireland). MAb was added in PBS containing 10% FCS and 0.1% nonionic detergent Tween 20, and bound MAb was detected with alkaline phosphatase-conjugated goat anti-human IgG (Sigma) followed by the addition of phosphatase substrate (Sigma). A_{405} measurements were taken using a microplate reader.

Construction of chimeric NL4-3/MOKW *env* proviruses. Chimeric proviruses were constructed from the pNL4-3 proviral plasmid (AIDS Research and Reference Reagent Program, National Institute of Allergy and Infectious Diseases) by overlapping PCR as previously described, with minor modifications (31). Briefly, the gp160 coding sequences were amplified from the cloning vectors using the primers EnvFv (5′-AGCAGAAGACAGTGGCAATGAGAGCGAAG-3′) and EnvR (5′-TTTTGACCACTTGCCACCCATCTTATAGC-3′). A portion of the NL4-3 provirus from nucleotides 5284 to 6232 was amplified with primers NL(5284)F (5′-GGTCAGGGAGTCTCCATAGAATGGAGG-3′) and NL(6232)Rv (5′-CTTCGCTCTCATTGCCACTGTCTTCTGCT-3′). This fragment encompasses the unique EcoRI restriction site in pNL4-3. Another fragment from the NL4-3 provirus spanning nucleotides 8779 to 9045 was amplified using the primers NL(8779)F (5′-GCTATAAGATGGGTGGCAAGTGGTCAAAA-3′) and NL(9045)R (5′-GATCTACAGCTGCCTTGTAAGTCATTGGTC-3′). This fragment includes the unique XhoI restriction site in pNL4-3. Overlapping PCR was used to join the gp160 coding sequence from the desired clone to the fragment encompassing bases 8779 to 9045 that had been amplified from pNL4-3. The resulting fragment was then similarly joined to the amplified fragment encompassing bases 5284 to 6232 from pNL4-3. The product was digested with EcoRI and XhoI and subcloned into the corresponding site in pBluescript SK(+) (Stratagene) for sequencing and subsequent manipulation. The EcoRI-XhoI fragment for each *env* gene was then subcloned back into pNL4-3. The results were proviral plasmids that differed from each other only in the *env* gene. The resulting plasmids were designated pNL-MOKW-RDL and pNL-MOKW-KNL.

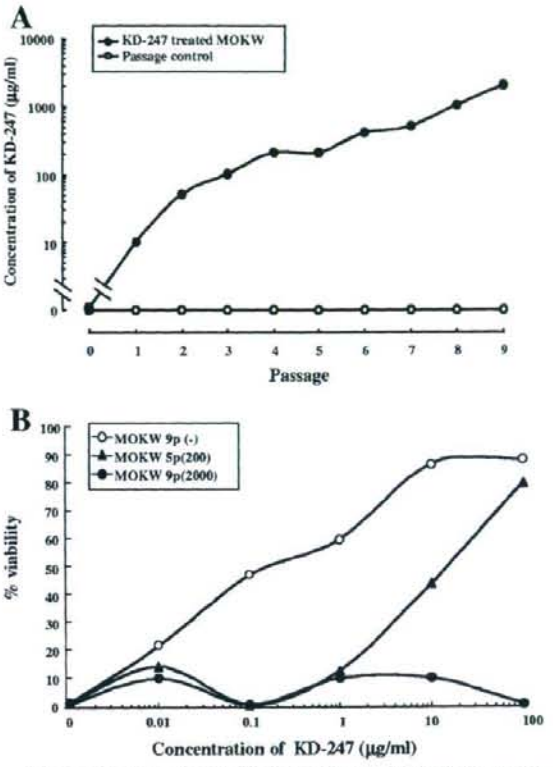

FIG. 1. Selection of neutralization-resistant virus variants against KD-247. (A) The selection was carried out in PM1/CCR5 cells, as described in Materials and Methods. (B) Sensitivity of MOKW5p(200) and MOKW9p(2000) virus to KD-247 as determined by MTT assay. PM1/CCR5 cells (2×10^3) were exposed to 100 $TCID_{50}$ of MOKW9p(−), MOKW5p(200), or MOKW9p(2000) virus and were cultured in the presence of various concentrations of KD-247. The IC_{50} values were determined by MTT assay on day 7 of culture. The assay was conducted in duplicate. The values shown are representative of three separate experiments.

Virus preparation and viral replication assay in PM1/CCR5 cells. Three micrograms of pNL-MOKW-RDL or pNL-MOKW-KNL was transfected into 293T cells using the Effectene transfection reagent. At 24 h after transfection, the virus-containing supernatants were harvested, filtered through a 0.2-μm-pore-size filter, and frozen in aliquots at −150°C. Viral yields were quantified by a RETROtek HIV-1 p24 antigen enzyme-linked immunosorbent assay (ELISA) kit (ZeptoMetrix). PM1/CCR5 cells (1×10^4) were exposed to NL4-3/MOKW *env* chimeric viruses corresponding to 10 ng of p24 and then preincubated for 4 h at 37°C. After incubation, cells were pelleted down and resuspended in RPMI 1640 medium supplemented with 10% FCS. Viral replication was monitored by measuring p24 kinetics in duplicate.

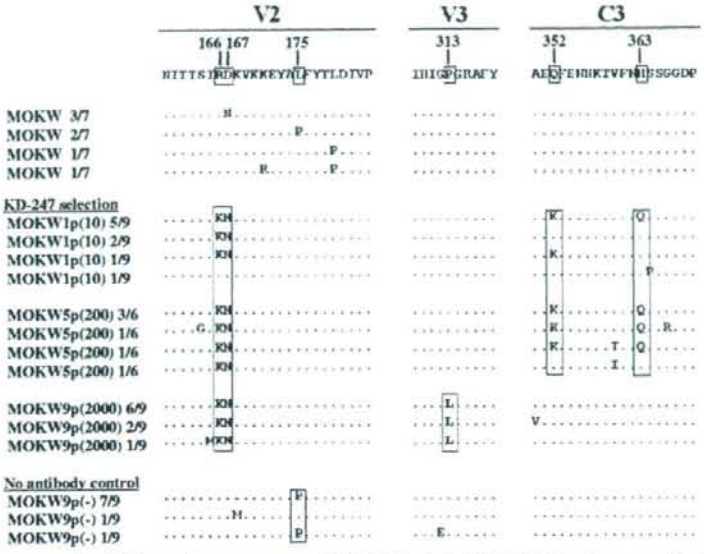

FIG. 2. Amino acid sequences of gp120 from the supernatants of MOKW-infected PM1/CCR5 cells passaged in the presence or absence of KD-247. Viral RNA from the cell culture supernatants at several concentrations of KD-247 was reverse transcribed. After the obtained cDNAs were subjected to PCR amplification and cloning, the *env* regions in the viruses passaged in the presence or absence of KD-247 were sequenced. The V2, V3, and C3 regions are indicated. The top amino acid sequence represents one of the major sequences from supernatants of MOKW-infected PBMCs. The locations and numbers of specific amino acids, based on the HXB2 sequence, are shown above the consensus line. The number of clones with the listed sequence among the total number of clones tested is given after each designation. For each set of clones, the deduced amino acid sequence of the gp120 was aligned by the single amino acid code. Dots denote sequence identity.

Nucleotide sequence accession numbers. Nucleotide sequences have been deposited in the DNA Data Bank of Japan under accession numbers AB262847 to AB262951 (passaged samples) and AB262952 to AB262961 (*env* expression vectors).

RESULTS

Anti-HIV-1 activity of KD-247 for the primary R5 isolate, MOKW virus. KD-247 recognized an epitope that contains the IGPGR sequence located at the tip of V3 and neutralized primary HIV-1 in clade B with matching sequence motifs (11). To study how bulked primary R5 virus can escape from anti-V3 antibody, we selected a genetically heterogenous HIV-1 primary isolate, MOKW, rather than a molecular clone to allow escape mutants to be selected from a quasi-species pool as well as to be generated de novo. MOKW virus was isolated by standard PBMC culture from a drug-naïve Japanese patient infected with HIV-1 by heterosexual contact (36). The isolate was sensitive to neutralization by KD-247 with a 50% inhibitory concentration (IC_{50}) of 3.4 μg/ml, which is comparable to the IC_{50} values of the Ba-L, JR-FL, and 89.6 viruses (data not shown).

Selection of KD-247 escape mutants from MOKW virus. To select an HIV-1 variant that could escape neutralization by KD-247 in vitro, we exposed PM1/CCR5 cells to MOKW virus and serially passaged the virus in the presence of increasing concentrations of KD-247. PM1/CCR5 cells were highly sensitive to both X4 and R5 HIV infection and were accompanied by prominent syncytia (68). As a control, MOKW virus was passaged under the same conditions but without KD-247 to allow us to monitor spontaneous changes that occurred in the virus during prolonged PM1/CCR5 cell passaging. The selected virus was initially propagated in the presence of 10 μg/ml KD-247, and during the course of the selection procedure, the MAb concentration was increased to 2,000 μg/ml (Fig. 1A). After five rounds of passaging, a viral variant, designated MOKW5p(200), arose that replicated in the presence of 200 μg of KD-247 per ml. Moreover, after nine rounds of passaging, a viral variant, designated MOKW9p(2000), arose that infected PM1/CCR5 cells efficiently in the presence of 2,000 μg/ml KD-247 (Fig. 1A). We harvested each passaged virus and a passaged control virus, designated MOKW9p(−), and evaluated their sensitivity to KD-247 using the MTT assay (Fig. 1B). The IC_{50} values of KD-247 against the MOKW9p(−), MOKW5p(200), and MOKW9p(2000) viruses were 0.15 μg/ml, 16 μg/ml, and >100 μg/ml, respectively, indicating that MOKW virus had acquired a resistance phenotype against KD-247 during the in vitro selection.

Sequences of the envelope region of the KD-247 escape mutants. To determine the genetic basis underlying the resistance of the variant MOKW strains, the *env* gene was amplified and sequenced. The C1 to C4 regions of the envelope were sequenced after cloning the PCR product for each region using cDNAs synthesized from viral RNAs obtained from the supernatants of infected cells, as previously described (67). A total of six to nine clones for each sample from PCR products from the passaged viruses were isolated and sequenced.

Before selection by KD-247 was begun, the V2 regions of MOKW *env* had variable amino acid sequences (Fig. 2). In

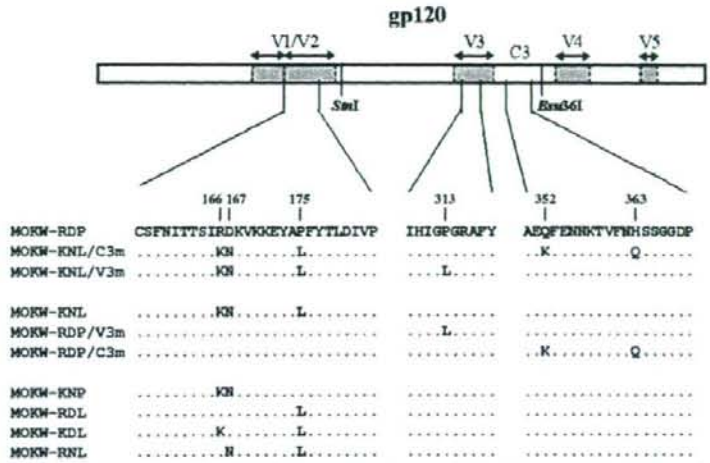

FIG. 3. Schematic representation of recombinant MOKW *env* genes used for analysis of the genetic basis for resistance to KD-247. MOKW-RDP, MOKW-KNL/C3m, and MOKW-KNL/V3m *env* genes were amplified from passaged MOKW virus-infected PM1/CCR5 cells in the absence or presence of KD-247. MOKW-KNL, MOKW-RDP/V3m, and MOKW-RDP/C3m *env* genes were constructed by replacing each region of MOKW-RDP with the corresponding MOKW-KNL/C3m or MOKW-KNL/V3m sequence. MOKW-KNP, MOKW-RDL, MOKW-KDL, and MOKW-RNL viruses were constructed by site-directed mutagenesis. Construction of the clones and mutagenesis procedures are described in Materials and Methods. The locations and numbers of specific amino acids, based on the HXB2 sequence, are shown above the MOKW-RDP sequence.

the first passage, two amino acid mutations in the V2 region and two amino acid mutations in the C3 region (five of nine clones) appeared, and after the fifth passage, the ratios of V2 and C3 mutated variants had further increased (seven of eight clones). However, after the ninth passage, the C3 mutations had completely disappeared, and a Pro-to-Leu substitution (P313L) in the V3 tip emerged in addition to the mutations in the V2 region (Fig. 2). The appearance of escape mutants with a V3 tip mutation was anticipated, because prior studies on the profile of KD-247 binding to peptides suggested that amino acid substitution at the V3 tip abrogates MAb binding (11). Some changes in the envelope sequence in other regions, including C1, V1, C2, V4, and C4, of the escape mutant were found even at early time points in the presence of the selective pressure. It is possible that these mutations also confer resistance to KD-247 but lead to viruses with decreased fitness, and thus they did not expand in the subsequent passage (Fig. 2 and data not shown). The virus passaged in PM1/CCR5 cells without KD-247 did not show the P313L substitution at passage 9 (zero of nine clones) (Fig. 2). However, accumulation of a mutation of leucine to proline at position 175 (L175P) in the V2 region was observed in the culture without KD-247. This mutation was not found in any passaged variants with KD-247.

Neutralization sensitivities of mutated MOKW pseudoviruses. To determine which substitutions were responsible for KD-247 resistance, we constructed luciferase-reporter viruses which were pseudotyped with the representative envelopes of MOKW5p(200), MOKW9p(2000), and passaged viruses without KD-247 [MOKW9p(−)], and were designated MOKW-KNL/C3m, MOKW-KNL/V3m, and MOKW-RDP virus, respectively (Fig. 3). Chimeric envelopes were constructed by replacing the mutated-region (V2, V3, or C3) with a corresponding MOKW-RDP virus (designated MOKW-KNL, MOKW-RDP/V3m, and MOKW-RDP/C3m, respectively), and then sensitivity was compared with that of the passaged virus without KD-247. As shown in Fig. 4, the V3-tip-mutated pseudoviruses, MOKW-KNL/V3m and MOKW-RDP/V3m, were completely resistant to KD-247 (>25,000-fold), whereas V2-mutated viruses, MOKW-KNL/C3m and MOKW-KNL, were only partially resistant (125-fold and 500-fold, respectively) (Fig. 4 and Table 1). The involvement in neutralization resistance of mutation in the V1/V2 region has been reported by number of researchers (12, 49, 50, 54). Our results show that the MOKW variants that had V2 mutations and a resistance phenotype against KD-247 were selected under pressure from relatively low concentrations of KD-247 (10 to 200 μg/ml) and that evolution of fully resistant variants with a mutation in the V3 tip was observed under pressure from high concentrations of the antibody.

We then determined whether the KD-247 escape variants remained sensitive to other neutralizing antibodies (447-52D and 17b), rsCD4, anti-CCR5 antibody (2D7), anti-CD4 antibody (RPA-T4), and the small-molecule CCR5 inhibitor (TAK-779) (Fig. 4 and Table 1). The KD-247 escape variants with the P313L mutation, MOKW-KNL/V3m and MOKW-RDP/V3m, were also resistant to another anti-V3 MAb, 447-52D, and V2-mutated viruses without V3 mutation, MOKW-KNL/C3m and MOKW-KNL, were partially resistant (the same as for KD-247). In contrast, the V2-mutated viruses (MOKW-KNL/C3m, MOKW-KNL/V3m, and MOKW-KNL) showed resistance to rsCD4 and 17b (a MAb to the CD4-induced epitope; CD4i) compared with the pseudoviruses without V2 mutations, i.e., MOKW-RDP, MOKW-RDP/C3m, and MOKW-RDP/V3m. Moreover, the pseudoviruses with V3 tip mutations, MOKW-KNL/V3m and MOKW-RDP/V3m, be-

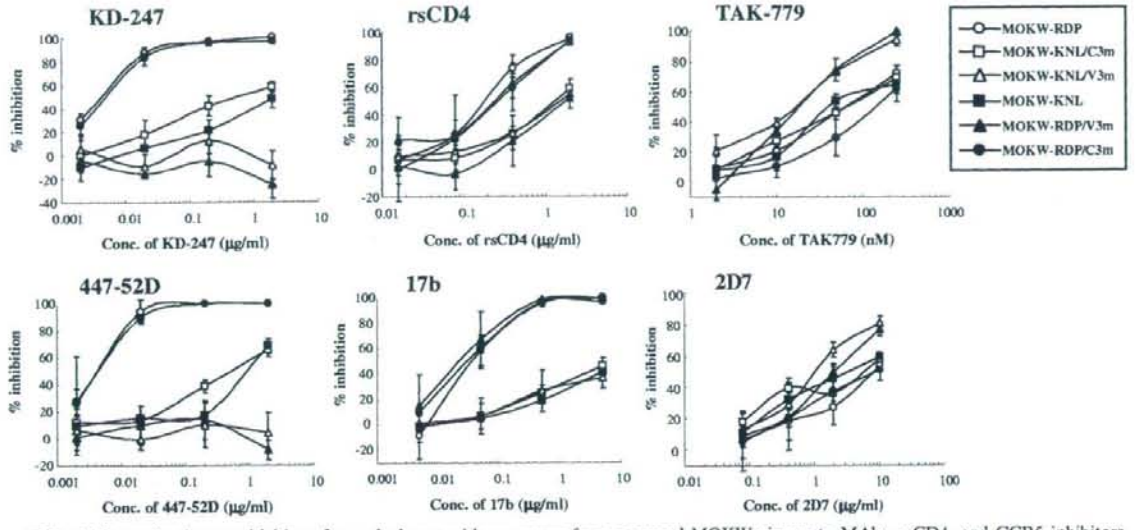

FIG. 4. Neutralization sensitivities of pseudoviruses with *env* genes from passaged MOKW viruses to MAbs, rsCD4, and CCR5 inhibitors. Pseudoviruses with the envelope sequences listed on the figure were prepared as described in Materials and Methods. KD-247, 447-52D, rsCD4, and 17b were preincubated with 100 $TCID_{50}$ of each MOKW pseudotype virus for 15 min, followed by the addition of the mixtures to the target cells (GHOST-hi5). The target cells were treated with TAK-779 and 2D7 for 15 min, followed by inoculation of the pseudotype clones. The inhibitory effects were determined by measuring the luciferase activities on day 2 of culture. Conc, concentration.

came significantly more sensitive to TAK-779 and 2D7 compared with pseudoviruses without the P313L mutation (Fig. 4 and Table 1). No significant differences with respect to sensitivity to RPA-T4 were observed between any pseudoviruses (Table 1). These data indicate that V3 tip and V2 mutations confer neutralization resistance against anti-V3 antibodies and that these mutations affect viral sensitivity to neutralizing antibodies recognizing different epitopes and anti-CCR5 antibody/agents.

Binding affinity of neutralizing antibodies to MOKW Env proteins on the cell surface. To elucidate the mechanism by which escape virus variants with V3 tip and V2 mutations become less sensitive to neutralizing antibodies, MOKW Env-expressing 293T cells were established by transfection with each Env expression plasmid and then stained with the MAbs. Binding of KD-247, 447-52D, and 17b to the surface-expressed Env proteins was assayed using fluorescence-activated cell sorter (FACS) analysis. As shown in Fig. 5A, the mean fluorescence intensities (MFIs) of KD-247 binding to the Env proteins without either V2 or V3 mutations (the MOKW-RDP and MOKW-RDP/C3m cells) were 30.13 and 29.20, respectively. However, the corresponding values for the V3-tip-mutated Env-expressing cells (MOKW-KNL/V3m and MOKW-RDP/V3m) were almost the same as negative controls (6.90 and 6.66, respectively). The MFI of the V2-mutated Env-expressing cells (MOKW-KNL/C3m and MOKW-KNL) indicated a lower binding affinity (17.89 and 19.18, respectively) than for Env proteins without V2 and V3 mutations. The binding pattern of 447-52D to these Env-expressing cells was similar to that of KD-247 (Fig. 5B). However, reduction in the binding of 17b was observed for strains with V2-mutated Env proteins (MOKW-KNL/C3m, MOKW-KNL/V3m, and

TABLE 1. Anti-HIV-1 activities of various MAbs and inhibitors toward MOKW pseudoviruses

Class	Compound	IC_{50} (μg/ml) of the indicated virus (relative IC_{50})[a]					
		MOKW-RDP	MOKW-KNL/C3m	MOKW-KNL/V3m	MOKW-RDP/C3m	MOKW-KNL	MOKW-RDP/V3m
V3 MAbs	KD-247	0.004 (1)	0.5 (125)	>100 (>25,000)	0.005 (1.3)	2 (500)	>100 (>25,000)
	447-52D	0.004 (1)	0.5 (125)	>2 (>500)	0.004 (1)	0.8 (200)	>2 (>500)
CD4-induced MAb	17b	0.035 (1)	>5 (>143)	>5 (>143)	0.03 (0.86)	>5 (>143)	0.02 (0.57)
CD4	rsCD4	0.18 (1)	1.3 (7.22)	1.5 (8.33)	0.24 (1.33)	1.8 (10)	0.24 (1.33)
CCR5 MAb	2D7	8 (1)	6.8 (0.85)	1 (0.13)	8 (1)	3.2 (0.4)	2 (0.25)
CCR5 inhibitor	TAK-779	63 (1)	63 (1)	18 (0.29)	140 (2.22)	65 (1)	18 (0.29)
CD4 MAb	RPA-T4	0.4 (1)	0.26 (0.65)	0.22 (0.55)	0.5 (1.25)	0.22 (0.55)	0.44 (1.1)

[a] GHOST-hi5 cells were exposed to 100 $TCID_{50}$ of each MOKW pseudovirus and then cultured in the presence of various concentrations of MAb or inhibitors. The IC_{50} values were determined using the luciferase reporter assay on day 2 of culture. All assays were conducted in triplicate. The value in parentheses is the ratio of the IC_{50} of the compound to the IC_{50} of the MOKW-RDP virus. Values for the compound TAK-779 are nanomolar concentrations. Data shown are representative of two or three separate experiments.

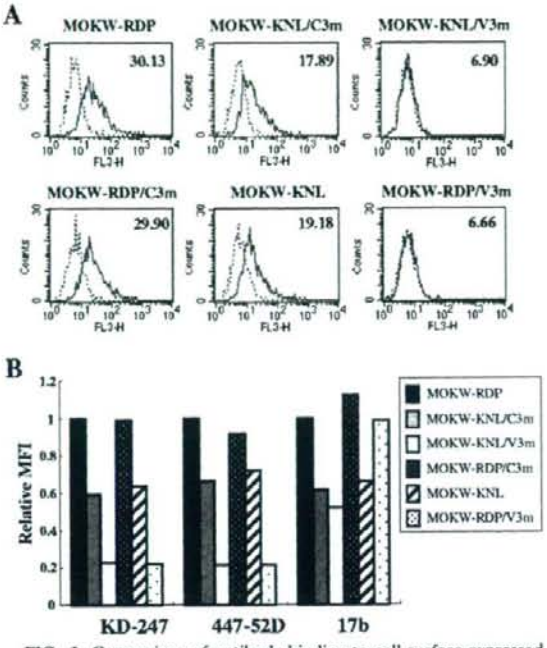

FIG. 5. Comparison of antibody binding to cell surface-expressed MOKW Env proteins. (A) 293T cells transfected with MOKW Env expression vectors were harvested at 24 h posttransfection and stained with KD-247. Flow cytometry data for binding of the KD-247 (black lines) to cell surface MOKW Env proteins are shown among GFP-gated 293T cells along with the control antibody (normal human IgG; dotted lines). The number at the top right of each graph is the MFI. (B) Each bar indicates the relative binding of KD-247, 447-52D, and 17b to MOKW Env-expressing cell surfaces. Data were normalized to each antibody's MFI for MOKW-RDP virus. FL3-H, relative fluorescence.

MOKW-KNL), whereas no difference in 17b binding was noted for the V3-mutants without V2 mutations (Fig. 5B). These findings are consistent with the results of a single-round neutralization assay (Fig. 4). Taken together, these data suggest that the mutations in V2 have a significant influence on access by antibodies to V3 as well as to the CD4i epitope. This is because access by antibodies to the epitopes of the functional envelope is related to neutralization sensitivity or resistance.

Identification of the V2 region site responsible for the neutralization resistance phenotype by site-directed mutagenesis of specific residues. Because KD-247 recognizes an epitope containing the IGPGR amino acid sequence in the V3 tip, the MAb could not bind the V3 tip of mutated Env proteins. Consequently, KD-247 does not neutralize V3-tip-mutated virus strains (67). However, the mechanism of neutralization resistance associated with V2 mutations is not known. To clarify the responsible mutation in the V2 region that confers the escape phenotype with respect to KD-247, we introduced V2 amino acid changes individually and in combination into the MOKW-RDP Env expression vector (Fig. 3) and measured the sensitivities of pseudoviruses with these envelopes to KD-247. As shown in Fig. 6, the R166K/D167N double mutant, MOKW-KNP virus, showed almost the same neutralization sensitivity as MOKW-RDP virus against KD-247. Surprisingly, a single amino acid change (P175L in MOKW-RDL) was sufficient to confer >10,000-fold resistance upon MOKW-RDP virus, with an IC_{50} of >100 μg/ml. R166K/P175L (MOKW-KDL) mutations also conferred resistance. Both the MOKW-RDL and MOKW-KDL viruses were much more resistant than the fully V2-mutated virus, MOKW-KNL (>100-fold and >10-fold resistance, respectively) (Fig. 6). The D167N/P175L (MOKW-RNL) mutant was more resistant than MOKW-KNL virus (10-fold) but less resistant than the MOKW-RDL and MOKW-KDL viruses. We also constructed a V2 mutant of JR-FL and confirmed that JR-FL with an amino acid substitution of Leu to Pro at position 175 became highly sensitive to KD-247 compared with JR-FL with Leu at position 175 in Env (data not shown). These results suggest that residue 175 (Pro or Leu) is the crucial amino acid for determining neutralization sensitivity against KD-247 and that the phenotypic influence of the R166K and D167N changes is strictly context dependent, requiring the presence of Leu at residue 175.

We then determined whether these pseudoviruses with various V2 mutations remained sensitive to other neutralizing antibodies (447-52D and IgGb12), rsCD4, 2D7, RPA-T4, and TAK-779 (Fig. 6). MOKW-RDL and MOKW-KDL viruses were also resistant to another anti-V3 MAb, 447-52D, CD4 binding site MAb, IgGb12, and rsCD4. MOKW-RNL was partially resistant compared with MOKW-KNL but less resistant than MOKW-RDL and MOKW-KDL against 447-52D, IgGb12, and rsCD4. These results were similar to those for KD-247. All V2-mutated clones were sensitive to TAK-779 and 2D7, as was MOKW-RDP virus (Fig. 6 and data not shown). However, the anti-CD4 MAb RPA-T4 neutralized both the MOKW-RDL and MOKW-KDL viruses at an approximately threefold lower concentration than other viruses (Fig. 6). These results suggest that the amino acids at positions 166 and 167 (with RD and KN sequences) may help compensate for any reduced fitness of viruses with Leu at residue 175. On the other hand, Pro at position 175 in MOKW-RDP virus might be accumulated because it confers better fitness to replicate on PM1/CCR5 cells in the absence of KD-247 pressure.

Binding affinity of MAbs against monomeric or cell surface-expressed gp120 with mutations in V2. To determine the difference in binding of MAbs to monomeric gp120 of MOKW Env with V2 mutations relative to that of MOKW-RDP virus, we performed MAb binding assays. Monomeric gp120 was prepared from pseudoviruses that had a series of V2 mutations and was captured on an ELISA plate, followed by detection by MAbs. No difference was noted in the binding activity of KD-247 or 447-52D to monomeric gp120 from V2-mutated and MOKW-RDP envelopes (Fig. 7). These results suggest that V2-mutated Env proteins retain the neutralizing epitope at least in monomeric gp120.

In contrast to the monomeric form, gp120 expressed on the cell surface contained, to a certain degree, functional envelope oligomers that were directly related to the infectivity and neutralization sensitivity of the virus. To compare the binding activity of MAbs for the surface-expressed Env with the results obtained for monomeric gp120, 293T cells transfected with MOKW-RDP and MOKW-KNP viruses, a V2 mutant strain, were subjected to FACS analysis. As shown in Fig. 8A and B,

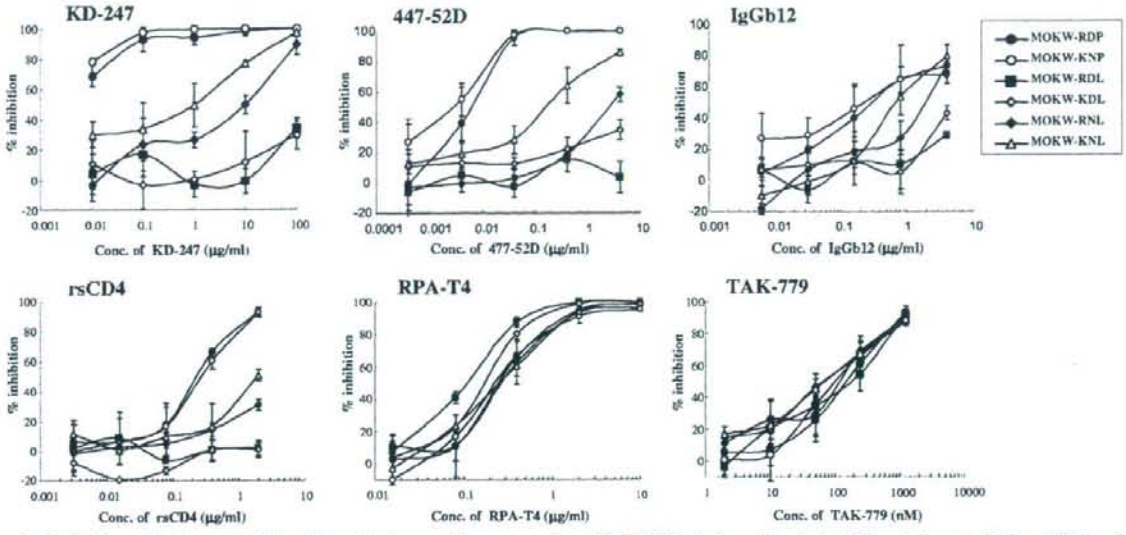

FIG. 6. Neutralization sensitivities of pseudoviruses with *env* genes from MOKW9C(−) virus with selected V2 mutations to MAbs, rsCD4, and CCR5 inhibitors. Pseudoviruses that have envelope sequences with the selected V2 mutations listed on Fig. 4 were prepared as described in Materials and Methods. KD-247, 447-52D, rsCD4, and IgGb12 were preincubated with 100 $TCID_{50}$ of each MOKW pseudotype virus for 15 min, followed by addition of the mixtures to the target cells (GHOST-hi5). Target cells were treated with TAK-779 and RPA-T4 for 15 min, followed by inoculation of the pseudotype clones. Inhibitory effects were determined by measuring the luciferase activities on day 2 of culture. Conc, concentration.

the relative binding of KD-247, 447-52D, and IgGb12 to Env expressed on the cell surface was no different than for MOKW-RDP and MOKW-KNP.

Consistent with the results of the single-round neutralization assay shown in Fig. 6, MOKW-RDL virus had the lowest binding affinity for all tested MAbs. To determine which mutations (166K or 167N) further influence binding affinity, in addition to the MOKW-RDL background, we constructed MOKW-KDL and MOKW-RNL Env proteins and measured the binding affinity by FACS. The MOKW-KDL Env was found to have a slightly greater binding affinity for KD-247, 447-52D, and IgGb12 than MOKW-RDL Env. But cell surface binding of all tested MAbs to MOKW-RNL was better than for MOKW-KDL. The strain with a fully V2-mutated Env, MOKW-KNL, had a binding profile that was intermediate between single- or double-mutated Env proteins and nonmutated Env, but in the case of IgGb12, the binding affinity of MAbs for MOKW-KNL was comparable to that for MOKW-RDP. These data were consistent with the results obtained from the neutralizing assay using a high concentration of each MAb (Fig. 6).

Comparison of replication kinetics between the NL-MOKW-RDL and NL-MOKW-KNL viruses. Although the MOKW-RDL variant was much more resistant against KD-247 than the MOKW-KNL variant (Fig. 6) and the RD sequence was

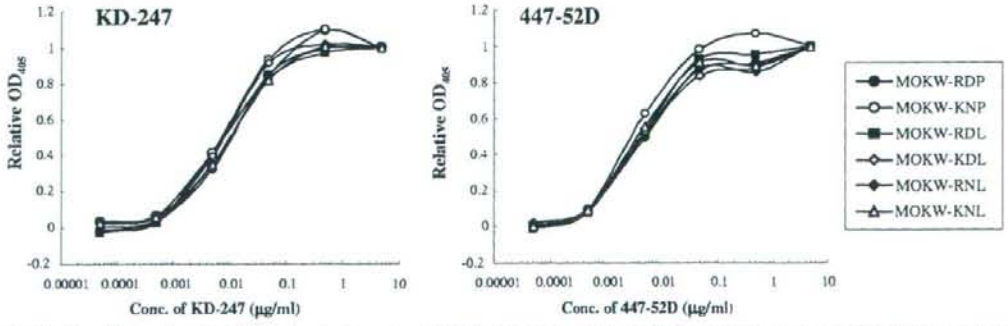

FIG. 7. Binding affinity of anti-V3 MAbs to monomeric gp120. Viral lysates for each MOKW pseudovirus were used. gp120 was captured onto microtiter wells using a sheep polyclonal antibody specific for the C terminus of gp120. Serial dilutions of KD-247 or 447-52D were tested for binding by ELISA. Because of differences in the amount of bound gp120, optical density at 405 nm (OD_{405}) values were normalized to saturating levels of antibody (5 μg/ml) for comparison. Conc, concentration.

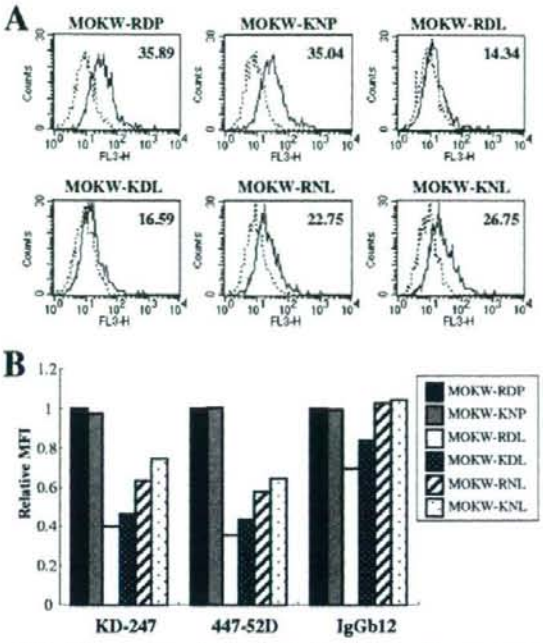

FIG. 8. Comparison of antibody binding to cell surface-expressed MOKW Env proteins with V2 mutations. (A) 293T cells transfected with MOKW Env-expression vectors were harvested at 24 h posttransfection and stained with KD-247. Flow cytometry data for binding of the KD-247 (black lines) to cell surface MOKW Env proteins are shown for GFP-gated 293T cells along with data for the control antibody (normal human IgG; dotted lines). The number at the top right of each graph is the MFI. (B) Each bar indicates relative binding of KD-247, 447-52D, and IgGb12 to MOKW Env-expressing cell surfaces. Data were normalized to each antibody's MFI for MOKW-RDP virus. FL3-H, relative fluorescence.

more prevalent than KN at positions 166 and 167 in the V2 region before selection (Fig. 2), the MOKW variants with 166K/167N/175L were selected and outgrown under KD-247 pressure (Fig. 2). It was possible that the KN sequences at positions 166 and 167 are necessary to compensate for the fitness of the variants with 175L in PM1/CCR5 cells, as shown in Fig. 6. To clarify the role of KN at positions 166 and 167 in replication, we constructed replication-competent viruses with a MOKW Env with RD or KN in addition to 175L (NL-MOKW-RDL and NL-MOKW-KNL) and compared their replication kinetics. As shown in Fig. 9, NL-MOKW-KNL virus replicated faster than NL-MOKW-RDL virus in PM1/CCR5 cells. These data suggested that KN sequences at positions 166 and 167 with the 175L variant confer a replication advantage in PM1/CCR5 cells. Therefore, the intermediate-resistant variant MOKW virus with the KNL sequence in the V2 region might replicate more rapidly than the highly resistant variant MOKW virus with RDL against KD-247 in the course of selection.

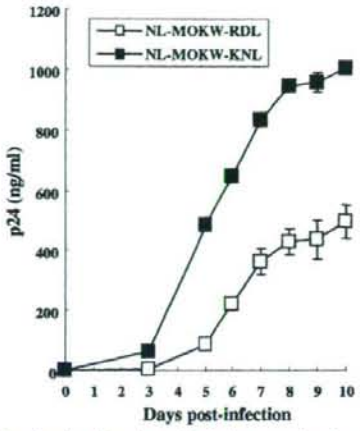

FIG. 9. Replication kinetics of infectious molecular clones NL-MOKW-RDL and NL-MOKW-KNL. PM1/CCR5 cells were exposed to NL-MOKW-RDL (open square) or NL-MOKW-KNL (filled square) and cultured for 10 days. Virus replication was monitored by measuring the amounts of p24 Gag protein produced in the culture supernatants. The data are representative of the results from two independent experiments.

DISCUSSION

Although an attack from the humoral immune response, especially anti-V3 NAb, is lasting against HIV-1 in vivo, it is not clear why the V3 tip sequence is conserved in the course of the infection. In the present study, by using a genetically heterogeneous HIV-1 primary R5 isolate, MOKW virus, we found that V2- and C3-mutated viruses expanded under conditions with a relatively low concentration of KD-247. Further, we found that the V3-tip-mutated virus was induced only under conditions with a high concentration of MAb (more than 500 μg/ml). Using region-swapping analysis, it was found that both V2 and V3 tip mutations can cause an escape phenotype against anti-V3 antibody. Neutralization escape variants with V2 mutations could be selected from quasi-species existing in the primary isolate at relatively low antibody pressures. On the other hand, highly resistant variants with amino acid substitutions in the V3 epitope emerged via evolution of the virus in the presence of a high concentration of the MAb.

The V1/V2 region of gp120 is highly diverse, not only in respect to virus subtypes but also in respect to intraspecies diversity in the same patient (16, 61, 66). The primary isolate, MOKW, also displayed diversity in the V2 region (Fig. 2), and the first-passaged virus already harbored mutations in the V2 region. Many researchers have reported that the V1/V2 domain strongly influences neutralization of the anti-V3 MAbs, MAbs to the other epitopes, and rsCD4 (12, 13, 25, 27, 30, 44, 49, 50). Moreover, structural models of the Env trimer have been proposed that place the base of the V1/V2 loop of one subunit in proximity to the V3 loop of a neighboring subunit (32, 34). In the present study we observed a reduction in the binding of anti-V3 MAbs to V2-mutated Env expressed on the cell surface, whereas mutations in V2 did not have an effect on the binding of the MAbs to monomeric gp120. These results suggest the association of V2 mutations with anti-V3 antibody

accessibility in the context of the oligomeric conformation of the functional envelope. It has been proposed that the gp120 of T-cell-line-adapted strains forms a relatively open conformation and that the primary isolate trimeric complex has a more closed conformation (2, 51). These findings suggest that antibody-induced V2 mutations may affect envelope oligomers on the viral surface so that they form a more closed conformation; thus, neutralization epitopes become less accessible to antibodies. The essential amino acid residues responsible for neutralization resistance located at the center of the V2 region may have a role in the interaction with the V3 loop of neighboring gp120 molecules.

We previously described the in vitro selection and characterization of a KD-247-escape mutant of JR-FL (67). The amino acid substitution that was critical for the resistance phenotype was Gly to Glu at residue 314 (G314E) in the V3 tip region. The genetically engineered mutant was completely resistant to neutralization by KD-247. Other researchers have also reported the induction of V3-mutated viruses by strain-specific anti-V3 MAb in in vitro culture systems (8, 37, 65). In earlier studies, combinations of genetically cloned viruses and highly potent NAbs were used for in vitro selection (8, 37, 65). The escape mutants were induced in the presence of high concentrations of MAbs to acquire V3 tip mutation(s). In contrast to these observations in vitro, the Gly-Pro-Gly amino acid sequence in the V3 tip varies to a negligible extent in clinical isolates from HIV-1-infected patients (35). The important role of the V3 tip in forming the β-turn of the V3 loop and in interacting with chemokine receptors may partly explain the discrepancy between in vivo and in vitro studies (19). In addition to the V3 loop, variation in or near the V1/V2 region is known to contribute to coreceptor usage of HIV-1 (17, 21, 27, 28, 47, 56, 64, 66). However, it is possible that HIV-1 suffers critical damage with respect to replication and infectivity through mutation in the V3 region, especially in the tip region, because the V3 loop plays a major role in the interaction of gp120 with coreceptors. Thus, mutations in the V2 region may be important not only to avoid anti-V3 pressure but also to maintain replication efficiency at a suitable level.

In the present study, which used a MOKW primary virus for selection, the virus underwent acquisition of resistance via V2 mutations and then V2 plus V3 mutations in response to increases in the concentration of MAb. By contrast, no V2 mutations were selected in JR-FL by KD-247 pressure in our previous study (67). Because MOKW was a primary isolate, the viruses contained quasi-species of related but distinct viruses, and relatively resistant variants with mutations in V2 were easily selected for replication. Pinter et al. found that inherent neutralization resistance in JR-FL is mediated by the V1/V2 domain (50). It is therefore possible that the V1/V2 sequence (or the conformation of this sequence) in JR-FL already had a resistance phenotype against anti-V3 antibodies because the escape variant underwent mutation directly in the V3 tip of the KD-247-reacting epitope (67).

In the in vitro selection process, amino acid residue 175 (Pro or Leu) in the V2 region of MOKW virus played a crucial role in dramatically changing the oligomeric state of the envelopes. However, MOKW-RDP obtained by prolonged culture in vitro without KD-247 became neutralization sensitive compared with MOKW virus. Residue 175P was the amino acid responsible for the change to the neutralization-sensitive phenotype, whereas viruses with 175L became highly resistant to the MAbs and rsCD4. The same phenomenon was observed in the relatively resistant strain JR-FL. Residue 175L is highly conserved among HIV-1 strains and is located at the center of the V2 loop (35), and the V2 region also mediates gp41-independent intersubunit contact (5). It is therefore possible that the V2 region, including residue 175, by mediating changes in the conformation of the gp120 oligomer, contributes to resistance to neutralization by limiting the exposure of epitopes.

Although the MOKW-RDL virus had a highly resistant phenotype against KD-247, MOKW virus with R166K/D167N and P175L in the V2 region and with the C3 mutations, which were less neutralization resistant than MOKW-RDL virus, were expanded in in vitro selection. Substitutions at residues 165 to 167 during the adaptation of various HIV-1 strains to replication in vitro have been reported; the adaptation is associated with an increase of the positive charge of this amino acid motif (1, 13, 39, 52, 57, 63). In our present study, the amino acid change at 166/167 in the V2 region in passaged MOKW viruses with KD-247 was RD to KN, again increasing the positive charge. MOKW-RDL virus was partially sensitive to anti-CD4 MAb (RPA-T4) compared with MOKW viruses with 175P, MOKW-RDP, and other 166/167-mutated MOKW viruses. Pugach et al. also showed that charged amino acids at residues 165 to 167 with 175L in the V2 region emerged during in vitro replication and that these viruses also had their sensitivity to rsCD4 and resistance to the anti-CD4 antibody slightly changed by the charged amino acids at positions 165 to 167 (52). It is therefore possible that amino acid mutations at positions 166 and 167 are necessary to compensate variants with 175L for interactions with CD4 molecules on the target cell membrane. As shown in Fig. 9, KN sequences at positions 166 and 167 with the 175L variant confer replication advantage in PM1/CCR5 cells. Therefore, residues 166 and 167 may help compensate for the reduced fitness of the viruses with Leu at position 175 in PM1/CCR5 cells. C3 mutations may also be involved in a minor compensation effect in replication cycles under moderate selective pressure from KD-247 (45, 60).

The neutralization resistance of primary HIV-1 variants is considered instrumental for HIV-1 persistence in the presence of NAbs in vivo. Various immunological pressures always induce escape variants by eliciting appropriate mutation(s) (14, 60, 62). In the present study, we found that HIV-1 could escape from the broadly reactive anti-V3 MAb, KD-247, by stepwise mutation in the V2 and V3 regions. These observations strongly support the idea that the major problem facing the development of V3-based immunogens is not sequence variation within V3 but, rather, that access of most V3-directed antibodies to their epitopes in functional Env complexes is blocked, often by the V1/V2 domain (29, 50).

Our observations support the hypothesis that neutralization escape in a primary isolate is mainly mediated by amino acid substitutions in the V2 region in vivo, because only a moderate selective pressure by neutralizing antibodies against autologous viruses has been reported for infected individuals (9, 14, 26, 50, 62). The large sequence diversity observed for V2 in quasi-species existing in patients may represent the accumulation of escape mutants early in HIV-1 infection in response to NAb pressure. Our observations may also explain why the V3

sequence in quasi-species existing in patients is relatively conserved in the face of a vigorous antibody response, especially in early HIV-1 infection. A recent study by Deeks et al. has important implications for understanding the NAb response against autologous virus (9): although NAb responses against contemporaneous autologous viruses are absent in early HIV infection, they can be detected at low levels in some patients with chronic infection. These data suggest the existence of an NAb response that overcomes the emergence of escape mutants. Further characterization of the response in humans who have potent and broadly neutralizing activities not affected by V1/V2 blocking effects may allow the identification of additional neutralization sites in HIV-1 Env, which might allow new targets to be identified for vaccine development.

ACKNOWLEDGMENTS

We are grateful to S. Zolla-Pazner of the New York University School of Medicine for providing MAb 447-52D and to Yasuhiro Kou for technical support. We also thank Yoko Kawanami for excellent technical assistance.

This work was supported in part by the Ministry of Health, Labor and Welfare of Japan (H-16-AIDS-001 and -012); a Grant-in aid for Scientific Research (C-18591119) from the Ministry of Education, Science and Culture of Japan; and the Cooperative Research Project on Clinical and Epidemiological Studies of Emerging and Re-emerging Infectious Diseases.

REFERENCES

1. **Bouma, P., M. Leavitt, P. F. Zhang, I. A. Sidorov, D. S. Dimitrov, and G. V. Quinnan, Jr.** 2003. Multiple interactions across the surface of the gp120 core structure determine the global neutralization resistance phenotype of human immunodeficiency virus type 1. J. Virol. **77:**8061–8071.
2. **Burton, D. R.** 1997. A vaccine for HIV type 1: the antibody perspective. Proc. Natl. Acad. Sci. USA **94:**10018–10023.
3. **Cao, Y., L. Qin, L. Zhang, J. Safrit, and D. D. Ho.** 1995. Virologic and immunologic characterization of long-term survivors of human immunodeficiency virus type 1 infection. N. Engl. J. Med. **332:**201–208.
4. **Carotenuto, P., D. Looij, L. Keldermans, F. de Wolf, and J. Goudsmit.** 1998. Neutralizing antibodies are positively associated with CD4+ T-cell counts and T-cell function in long-term AIDS-free infection. AIDS **12:**1591–1600.
5. **Center, R. J., P. L. Earl, J. Lebowitz, P. Schuck, and B. Moss.** 2000. The human immunodeficiency virus type 1 gp120 V2 domain mediates gp41-independent intersubunit contacts. J. Virol. **74:**4448–4455.
6. **Center, R. J., R. D. Leapman, J. Lebowitz, L. O. Arthur, P. L. Earl, and B. Moss.** 2002. Oligomeric structure of the human immunodeficiency virus type 1 envelope protein on the virion surface. J. Virol. **76:**7863–7867.
7. **Cole, K. S., J. D. Steckbeck, J. L. Rowles, R. C. Desrosiers, and R. C. Montelaro.** 2004. Removal of N-linked glycosylation sites in the V1 region of simian immunodeficiency virus gp120 results in redirection of B-cell responses to V3. J. Virol. **78:**1525–1539.
8. **D'Costa, S., K. S. Slobod, R. G. Webster, S. W. White, and J. L. Hurwitz.** 2001. Structural features of HIV envelope defined by antibody escape mutant analysis. AIDS Res. Hum. Retrovir. **17:**1205–1209.
9. **Deeks, S. G., B. Schweighardt, T. Wrin, J. Galovich, R. Hoh, E. Sinclair, P. Hunt, J. M. McCune, J. N. Martin, C. J. Petropoulos, and F. M. Hecht.** 2006. Neutralizing antibody responses against autologous and heterologous viruses in acute versus chronic human immunodeficiency virus (HIV) infection: evidence for a constraint on the ability of HIV to completely evade neutralizing antibody responses. J. Virol. **80:**6155–6164.
10. **Eda, Y., T. Murakami, Y. Ami, T. Nakasone, M. Takizawa, K. Someya, M. Kaizu, Y. Izumi, N. Yoshino, S. Matsushita, H. Higuchi, H. Matsui, K. Shinohara, H. Takeuchi, Y. Koyanagi, N. Yamamoto, and M. Honda.** 2006. Anti-V3 humanized antibody KD-247 effectively suppresses ex vivo generation of human immunodeficiency virus type 1 and affords sterile protection of monkeys against a heterologous simian/human immunodeficiency virus infection. J. Virol. **80:**5563–5570.
11. **Eda, Y., M. Takizawa, T. Murakami, H. Maeda, K. Kimachi, H. Yonemura, S. Koyanagi, K. Shiosaki, H. Higuchi, K. Makizumi, T. Nakashima, K. Osatomi, S. Tokiyoshi, S. Matsushita, N. Yamamoto, and M. Honda.** 2006. Sequential immunization with V3 peptides from primary human immunodeficiency virus type 1 produces cross-neutralizing antibodies against primary isolates with a matching narrow-neutralization sequence motif. J. Virol. **80:**5552–5562.
12. **Etemad-Moghadam, B., Y. Sun, E. K. Nicholson, G. B. Karlsson, D. Schenten, and J. Sodroski.** 1999. Determinants of neutralization resistance in the envelope glycoproteins of a simian-human immunodeficiency virus passaged in vivo. J. Virol. **73:**8873–8879.
13. **Follis, K. E., M. Trahey, R. A. LaCasse, and J. H. Nunberg.** 1998. Continued utilization of CCR5 coreceptor by a newly derived T-cell line-adapted isolate of human immunodeficiency virus type 1. J. Virol. **72:**7603–7608.
14. **Frost, S. D., T. Wrin, D. M. Smith, S. L. Kosakovsky Pond, Y. Liu, E. Paxinos, C. Chappey, J. Galovich, J. Beauchaine, C. J. Petropoulos, S. J. Little, and D. D. Richman.** 2005. Neutralizing antibody responses drive the evolution of human immunodeficiency virus type 1 envelope during recent HIV infection. Proc. Natl. Acad. Sci. USA **102:**18514–18519.
15. **Gorny, M. K., K. Revesz, C. Williams, B. Volsky, M. K. Louder, C. A. Anyangwe, C. Krachmarov, S. C. Kayman, A. Pinter, A. Nadas, P. N. Nyambi, J. R. Mascola, and S. Zolla-Pazner.** 2004. The V3 loop is accessible on the surface of most human immunodeficiency virus type 1 primary isolates and serves as a neutralization epitope. J. Virol. **78:**2394–2404.
16. **Groenink, M., R. A. Fouchier, S. Broersen, C. H. Baker, M. Koot, A. B. van't Wout, H. G. Huisman, F. Miedema, M. Tersmette, and H. Schuitemaker.** 1993. Relation of phenotype evolution of HIV-1 to envelope V2 configuration. Science **260:**1513–1516.
17. **Harrowe, G., and C. Cheng-Mayer.** 1995. Amino acid substitutions in the V3 loop are responsible for adaptation to growth in transformed T-cell lines of a primary human immunodeficiency virus type 1. Virology **210:**490–494.
18. **Hope, T. J., X. J. Huang, D. McDonald, and T. G. Parslow.** 1990. Steroid-receptor fusion of the human immunodeficiency virus type 1 Rev transactivator: mapping cryptic functions of the arginine-rich motif. Proc. Natl. Acad. Sci. USA **87:**7787–7791.
19. **Hu, Q., J. O. Trent, G. D. Tomaras, Z. Wang, J. L. Murray, S. M. Conolly, J. M. Navenot, A. P. Barry, M. L. Greenberg, and S. C. Peiper.** 2000. Identification of ENV determinants in V3 that influence the molecular anatomy of CCR5 utilization. J. Mol. Biol. **302:**359–375.
20. **Huang, C. C., M. Tang, M. Y. Zhang, S. Majeed, E. Montabana, R. L. Stanfield, D. S. Dimitrov, B. Korber, J. Sodroski, I. A. Wilson, R. Wyatt, and P. D. Kwong.** 2005. Structure of a V3-containing HIV-1 gp120 core. Science **310:**1025–1028.
21. **Hwang, S. S., T. J. Boyle, H. K. Lyerly, and B. R. Cullen.** 1991. Identification of the envelope V3 loop as the primary determinant of cell tropism in HIV-1. Science **253:**71–74.
22. **Jacobson, J. M., N. Colman, N. A. Ostrow, R. W. Simson, D. Tomesch, L. Marlin, M. Rao, J. L. Mills, J. Clemens, and A. M. Prince.** 1993. Passive immunotherapy in the treatment of advanced human immunodeficiency virus infection. J. Infect. Dis. **168:**298–305.
23. **Javaherian, K., A. J. Langlois, C. McDanal, K. L. Ross, L. I. Eckler, C. L. Jellis, A. T. Profy, J. R. Rusche, D. P. Bolognesi, S. D. Putney, et al.** 1989. Principal neutralizing domain of the human immunodeficiency virus type 1 envelope protein. Proc. Natl. Acad. Sci. USA **86:**6768–6772.
24. **Johnson, W. E., and R. C. Desrosiers.** 2002. Viral persistance: HIV's strategies of immune system evasion. Annu. Rev. Med. **53:**499–518.
25. **Kang, S. M., F. S. Quan, C. Huang, L. Guo, L. Ye, C. Yang, and R. W. Compans.** 2005. Modified HIV envelope proteins with enhanced binding to neutralizing monoclonal antibodies. Virology **331:**20–32.
26. **Kimura, T., K. Yoshimura, K. Nishihara, Y. Maeda, S. Matsumi, A. Koito, and S. Matsushita.** 2002. Reconstitution of spontaneous neutralizing antibody response against autologous human immunodeficiency virus during highly active antiretroviral therapy. J. Infect. Dis. **185:**53–60.
27. **Koito, A., G. Harrowe, J. A. Levy, and C. Cheng-Mayer.** 1994. Functional role of the V1/V2 region of human immunodeficiency virus type 1 envelope glycoprotein gp120 in infection of primary macrophages and soluble CD4 neutralization. J. Virol. **68:**2253–2259.
28. **Koito, A., L. Stamatatos, and C. Cheng-Mayer.** 1995. Small amino acid sequence changes within the V2 domain can affect the function of a T-cell line-tropic human immunodeficiency virus type 1 envelope gp120. Virology **206:**878–884.
29. **Krachmarov, C., A. Pinter, W. J. Honnen, M. K. Gorny, P. N. Nyambi, S. Zolla-Pazner, and S. C. Kayman.** 2005. Antibodies that are cross-reactive for human immunodeficiency virus type 1 clade A and clade B V3 domains are common in patient sera from Cameroon, but their neutralization activity is usually restricted by epitope masking. J. Virol. **79:**780–790.
30. **Krachmarov, C. P., W. J. Honnen, S. C. Kayman, M. K. Gorny, S. Zolla-Pazner, and A. Pinter.** 2006. Factors determining the breadth and potency of neutralization by V3-specific human monoclonal antibodies derived from subjects infected with clade A or clade B strains of human immunodeficiency virus type 1. J. Virol. **80:**7127–7135.
31. **Kuhmann, S. E., P. Pugach, K. J. Kunstman, J. Taylor, R. L. Stanfield, A. Snyder, J. M. Strizki, J. Riley, B. M. Baroudy, I. A. Wilson, B. T. Korber, S. M. Wolinsky, and J. P. Moore.** 2004. Genetic and phenotypic analyses of human immunodeficiency virus type 1 escape from a small-molecule CCR5 inhibitor. J. Virol. **78:**2790–2807.
32. **Kwong, P. D., M. L. Doyle, D. J. Casper, C. Cicala, S. A. Leavitt, S. Majeed, T. D. Steenbeke, M. Venturi, I. Chaiken, M. Fung, H. Katinger, P. W. Parren, J. Robinson, D. Van Ryk, L. Wang, D. R. Burton, E. Freire, R. Wyatt, J. Sodroski, W. A. Hendrickson, and J. Arthos.** 2002. HIV-1 evades anti-

body-mediated neutralization through conformational masking of receptor-binding sites. Nature **420**:678–682.
33. **Kwong, P. D., R. Wyatt, J. Robinson, R. W. Sweet, J. Sodroski, and W. A. Hendrickson.** 1998. Structure of an HIV gp120 envelope glycoprotein in complex with the CD4 receptor and a neutralizing human antibody. Nature **393**:648–659.
34. **Kwong, P. D., R. Wyatt, Q. J. Sattentau, J. Sodroski, and W. A. Hendrickson.** 2000. Oligomeric modeling and electrostatic analysis of the gp120 envelope glycoprotein of human immunodeficiency virus. J. Virol. **74**:1961–1972.
35. **Leitner, T., B. Foley, B. Hahn, P. Marx, F. McCutchan, J. Mellors, S. Wolinsky, and B. Korber.** 2005. HIV sequence compendium 2005. LA-UR 06-0680. Theoretical Biology and Biophysics Group, Los Alamos National Laboratory, Los Alamos, NM.
36. **Maeda, K., K. Yoshimura, S. Shibayama, H. Habashita, H. Tada, K. Sagawa, T. Miyakawa, M. Aoki, D. Fukushima, and H. Mitsuya.** 2001. Novel low molecular weight spirodiketopiperazine derivatives potently inhibit R5 HIV-1 infection through their antagonistic effects on CCR5. J. Biol. Chem. **276**:35194–35200.
37. **Masuda, T., S. Matsushita, M. J. Kuroda, M. Kannagi, K. Takatsuki, and S. Harada.** 1990. Generation of neutralization-resistant HIV-1 in vitro due to amino acid interchanges of third hypervariable env region. J. Immunol. **145**:3240–3246.
38. **McCaffrey, R. A., C. Saunders, M. Hensel, and L. Stamatatos.** 2004. N-Linked glycosylation of the V3 loop and the immunologically silent face of gp120 protects human immunodeficiency virus type 1 SF162 from neutralization by anti-gp120 and anti-gp41 antibodies. J. Virol. **78**:3279–3295.
39. **Mo, H., L. Stamatatos, J. E. Ip, C. F. Barbas, P. W. Parren, D. R. Burton, J. P. Moore, and D. D. Ho.** 1997. Human immunodeficiency virus type 1 mutants that escape neutralization by human monoclonal antibody IgG1b12. off. J. Virol. **71**:6869–6874.
40. **Montefiori, D. C., T. S. Hill, H. T. Vo, B. D. Walker, and E. S. Rosenberg.** 2001. Neutralizing antibodies associated with viremia control in a subset of individuals after treatment of acute human immunodeficiency virus type 1 infection. J. Virol. **75**:10200–10207.
41. **Moore, J. P., Y. Cao, D. D. Ho, and R. A. Koup.** 1994. Development of the anti-gp120 antibody response during seroconversion to human immunodeficiency virus type 1. J. Virol. **68**:5142–5155.
42. **Moore, J. P., Y. Cao, L. Qing, Q. J. Sattentau, J. Pyati, R. Koduri, J. Robinson, C. F. Barbas III, D. R. Burton, and D. D. Ho.** 1995. Primary isolates of human immunodeficiency virus type 1 are relatively resistant to neutralization by monoclonal antibodies to gp120, and their neutralization is not predicted by studies with monomeric gp120. J. Virol. **69**:101–109.
43. **Moore, J. P., and D. D. Ho.** 1993. Antibodies to discontinuous or conformationally sensitive epitopes on the gp120 glycoprotein of human immunodeficiency virus type 1 are highly prevalent in sera of infected humans. J. Virol. **67**:863–875.
44. **Morikita, T., Y. Maeda, S. Fujii, S. Matsushita, K. Obaru, and K. Takatsuki.** 1997. The V1/V2 region of human immunodeficiency virus type 1 modulates the sensitivity to neutralization by soluble CD4 and cellular tropism. AIDS Res. Hum. Retrovir. **13**:1291–1299.
45. **Otto, C., B. A. Puffer, S. Pohlmann, R. W. Doms, and F. Kirchhoff.** 2003. Mutations in the C3 region of human and simian immunodeficiency virus envelope have differential effects on viral infectivity, replication, and CD4-dependency. Virology **315**:292–302.
46. **Park, E. J., L. K. Vujcic, R. Anand, T. S. Theodore, and G. V. Quinnan, Jr.** 1998. Mutations in both gp120 and gp41 are responsible for the broad neutralization resistance of variant human immunodeficiency virus type 1 MN to antibodies directed at V3 and non-V3 epitopes. J. Virol. **72**:7099–7107.
47. **Pastore, C., R. Nedellec, A. Ramos, S. Pontow, L. Ratner, and D. E. Mosier.** 2006. Human immunodeficiency virus type 1 coreceptor switching: V1/V2 gain-of-fitness mutations compensate for V3 loss-of-fitness mutations. J. Virol. **80**:750–758.
48. **Pilgrim, A. K., G. Pantaleo, O. J. Cohen, L. M. Fink, J. Y. Zhou, J. T. Zhou, D. P. Bolognesi, A. S. Fauci, and D. C. Montefiori.** 1997. Neutralizing antibody responses to human immunodeficiency virus type 1 in primary infection and long-term-nonprogressive infection. J. Infect. Dis. **176**:924–932.
49. **Pinter, A., W. J. Honnen, P. D'Agostino, M. K. Gorny, S. Zolla-Pazner, and S. C. Kayman.** 2005. The C108g epitope in the V2 domain of gp120 functions as a potent neutralization target when introduced into envelope proteins derived from human immunodeficiency virus type 1 primary isolates. J. Virol. **79**:6909–6917.
50. **Pinter, A., W. J. Honnen, Y. He, M. K. Gorny, S. Zolla-Pazner, and S. C. Kayman.** 2004. The V1/V2 domain of gp120 is a global regulator of the sensitivity of primary human immunodeficiency virus type 1 isolates to neutralization by antibodies commonly induced upon infection. J. Virol. **78**: 5205–5215.
51. **Poignard, P., E. O. Saphire, P. W. Parren, and D. R. Burton.** 2001. gp120: biologic aspects of structural features. Annu. Rev. Immunol. **19**:253–274.
52. **Pugach, P., S. E. Kuhmann, J. Taylor, A. J. Marozsan, A. Snyder, T. Ketas, S. M. Wolinsky, B. T. Korber, and J. P. Moore.** 2004. The prolonged culture of human immunodeficiency virus type 1 in primary lymphocytes increases its sensitivity to neutralization by soluble CD4. Virology **321**:8–22.
53. **Sakaguchi, N., T. Kimura, S. Matsushita, S. Fujimura, J. Shibata, M. Araki, T. Sakamoto, C. Minoda, and K. Kuwahara.** 2005. Generation of high-affinity antibody against T cell-dependent antigen in the Ganp gene-transgenic mouse. J. Immunol. **174**:4485–4494.
54. **Saunders, C. J., R. A. McCaffrey, I. Zharkikh, Z. Kraft, S. E. Malenbaum, B. Burke, C. Cheng-Mayer, and L. Stamatatos.** 2005. The V1, V2, and V3 regions of the human immunodeficiency virus type 1 envelope differentially affect the viral phenotype in an isolate-dependent manner. J. Virol. **79**:9069–9080.
55. **Sawyer, L. S., M. T. Wrin, L. Crawford-Miksza, B. Potts, Y. Wu, P. A. Weber, R. D. Alfonso, and C. V. Hanson.** 1994. Neutralization sensitivity of human immunodeficiency virus type 1 is determined in part by the cell in which the virus is propagated. J. Virol. **68**:1342–1349.
55a. **Shibata, J., K. Yoshimura, A. Honda, A. Koito, T. Murakami, and S. Matsusushita.** 2006. A role of mutations in non-V3 envelope regions for escape from a broad neutralizing anti-V3 monoclonal antibody, KD-247, during in vitro selection, abstr. 415. 13th Conf. Retrovir. Opportunistic Infect., Denver, CO, 5 to 8 February 2006.
56. **Shioda, T., J. A. Levy, and C. Cheng-Mayer.** 1992. Small amino acid changes in the V3 hypervariable region of gp120 can affect the T-cell-line and macrophage tropism of human immunodeficiency virus type 1. Proc. Natl. Acad. Sci. USA **89**:9434–9438.
57. **Sullivan, N., M. Thali, C. Furman, D. D. Ho, and J. Sodroski.** 1993. Effect of amino acid changes in the V1/V2 region of the human immunodeficiency virus type 1 gp120 glycoprotein on subunit association, syncytium formation, and recognition by a neutralizing antibody. J. Virol. **67**:3674–3679.
58. **Trkola, A., H. Kuster, P. Rusert, B. Joos, M. Fischer, C. Leemann, A. Manrique, M. Huber, M. Rehr, A. Oxenius, R. Weber, G. Stiegler, B. Vcelar, H. Katinger, L. Aceto, and H. F. Gunthard.** 2005. Delay of HIV-1 rebound after cessation of antiretroviral therapy through passive transfer of human neutralizing antibodies. Nat. Med. **11**:615–622.
59. **Trkola, A., A. B. Pomales, H. Yuan, B. Korber, P. J. Maddon, G. P. Allaway, H. Katinger, C. F. Barbas III, D. R. Burton, D. D. Ho, et al.** 1995. Cross-clade neutralization of primary isolates of human immunodeficiency virus type 1 by human monoclonal antibodies and tetrameric CD4-IgG. J. Virol. **69**:6609–6617.
60. **Wang, F. X., T. Kimura, K. Nishihara, K. Yoshimura, A. Koito, and S. Matsushita.** 2002. Emergence of autologous neutralization-resistant variants from preexisting human immunodeficiency virus (HIV) quasi species during virus rebound in HIV type 1-infected patients undergoing highly active antiretroviral therapy. J. Infect. Dis. **185**:608–617.
61. **Wang, N., T. Zhu, and D. D. Ho.** 1995. Sequence diversity of V1 and V2 domains of gp120 from human immunodeficiency virus type 1: lack of correlation with viral phenotype. J. Virol. **69**:2708–2715.
62. **Wei, X., J. M. Decker, S. Wang, H. Hui, J. C. Kappes, X. Wu, J. F. Salazar-Gonzalez, M. G. Salazar, J. M. Kilby, M. S. Saag, N. L. Komarova, M. A. Nowak, B. H. Hahn, P. D. Kwong, and G. M. Shaw.** 2003. Antibody neutralization and escape by HIV-1. Nature **422**:307–312.
63. **Wrin, T., T. P. Loh, J. C. Vennari, H. Schuitemaker, and J. H. Nunberg.** 1995. Adaptation to persistent growth in the H9 cell line renders a primary isolate of human immunodeficiency virus type 1 sensitive to neutralization by vaccine sera. J. Virol. **69**:39–48.
64. **Wyatt, R., J. Moore, M. Accola, E. Desjardin, J. Robinson, and J. Sodroski.** 1995. Involvement of the V1/V2 variable loop structure in the exposure of human immunodeficiency virus type 1 gp120 epitopes induced by receptor binding. J. Virol. **69**:5723–5733.
65. **Yoshida, K., M. Nakamura, and T. Ohno.** 1997. Mutations of the HIV type 1 V3 loop under selection pressure with neutralizing monoclonal antibody NM-01. AIDS Res. Hum. Retrovir. **13**:1283–1290.
66. **Yoshimura, K., S. Matsushita, A. Hayashi, and K. Takatsuki.** 1996. Relationship of HIV-1 envelope V2 and V3 sequences of the primary isolates to the viral phenotype. Microbiol. Immunol. **40**:277–287.
67. **Yoshimura, K., J. Shibata, T. Kimura, A. Honda, Y. Maeda, A. Koito, T. Murakami, H. Mitsuya, and S. Matsushita.** 2006. Resistance profile of a novel broadly neutralizing anti-HIV monoclonal antibody, KD-247, that shows favorable synergism with anti-CCR5 inhibitors in vitro. AIDS **20**: 2065–2073.
68. **Yusa, K., Y. Maeda, A. Fujioka, K. Monde, and S. Harada.** 2005. Isolation of TAK-779-resistant HIV-1 from an R5 HIV-1 gp120 V3 loop library. J. Biol. Chem. **280**:30083–30090.
69. **Zolla-Pazner, S.** 2004. Identifying epitopes of HIV-1 that induce protective antibodies. Nat. Rev. Immunol. **4**:199–210.

THE JOURNAL OF BIOLOGICAL CHEMISTRY VOL. 281, NO. 18, pp. 12688–12698, May 5, 2006
Printed in the U.S.A.

Structural and Molecular Interactions of CCR5 Inhibitors with CCR5*

Received for publication, November 28, 2005, and in revised form, January 25, 2006 Published, JBC Papers in Press, February 23, 2006, DOI 10.1074/jbc.M512688200

Kenji Maeda[‡§¶], Debananda Das[¶], Hiromi Ogata-Aoki[‡§], Hirotomo Nakata[‡§], Toshikazu Miyakawa[§], Yasushi Tojo[‡§], Rachael Norman[¶], Yoshikazu Takaoka[‖], Jianping Ding[**], Gail F. Arnold[**], Eddy Arnold[**], and Hiroaki Mitsuya[‡§¶1]

From the [‡]Department of Hematology and [§]Department of Infectious Diseases, Kumamoto University Graduate School of Medical and Pharmaceutical Sciences, Kumamoto 860-8556, Japan, the [¶]Experimental Retrovirology Section, HIV and AIDS Malignancy Branch, NCI, National Institutes of Health, Bethesda, Maryland 20892, the [‖]Minase Research Institute, Ono Pharmaceutical Co. Ltd., Osaka 618-8585, Japan, and the [**]Center for Advanced Biotechnology and Medicine, and Chemistry and Chemical Biology Department, Rutgers University, Piscataway, New Jersey 08854

We have characterized the structural and molecular interactions of CC-chemokine receptor 5 (CCR5) with three CCR5 inhibitors active against R5 human immunodeficiency virus type 1 (HIV-1) including the potent *in vitro* and *in vivo* CCR5 inhibitor aplaviroc (AVC). The data obtained with saturation binding assays and structural analyses delineated the key interactions responsible for the binding of CCR5 inhibitors with CCR5 and illustrated that their binding site is located in a predominantly lipophilic pocket in the interface of extracellular loops and within the upper transmembrane (TM) domain of CCR5. Mutations in the CCR5 binding sites of AVC decreased gp120 binding to CCR5 and the susceptibility to HIV-1 infection, although mutations in TM4 and TM5 that also decreased gp120 binding and HIV-1 infectivity had less effects on the binding of CC-chemokines, suggesting that CCR5 inhibition targeting appropriate regions might render the inhibition highly HIV-1-specific while preserving the CC chemokine-CCR5 interactions. The present data delineating residue by residue interactions of CCR5 with CCR5 inhibitors should not only help design more potent and more HIV-1-specific CCR5 inhibitors, but also give new insights into the dynamics of CC-chemokine-CCR5 interactions and the mechanisms of CCR5 involvement in the process of cellular entry of HIV-1.

Highly active antiretroviral therapy has brought about a major impact on the acquired immunodeficiency syndrome (AIDS) epidemics in industrially advanced nations (1, 2), however, eradication of HIV-1[2] appears to be currently impossible mainly because of the viral reservoirs remaining in blood and infected tissues (3). Successful antiviral drugs, in theory, exert their virus-specific effects by interacting with viral components such as viral genes or their transcripts without disturbing cellular metabolisms or functions (2). However, at present, no antiretroviral drugs or agents have been demonstrated to be completely specific for HIV-1 and devoid of toxicity or side effects in the therapy of AIDS (4). Limitations of antiviral therapy of AIDS are exacerbated by complicated regimens, emergence of drug-resistant HIV-1 variants (1), and a number of inherent adverse effects (5).

Thus, identification of new antiretroviral drugs that have unique mechanisms of action and produce no or least minimal side effects remains an important therapeutic objective (2, 4). CCR5 is a member of the G protein-coupled, seven-transmembrane segment receptors, which comprise the largest superfamily of proteins in the body (6). In 1996, it was revealed that CCR5 serves as one of the two essential coreceptors for HIV-1 entry to human $CD4^+$ cells, thereby serving as an attractive target for possible intervention of HIV-1 infection (7–10). Aplaviroc (AVC; AK602/ONO4128/873140; Fig. 1), a novel spirodiketopiperazine derivative, represents a CCR5 inhibitor that specifically binds to human CCR5 with a high affinity, greatly blocks HIV-1-gp120/CCR5 binding, and exerts potent activity against a wide spectrum of laboratory and primary R5-HIV-1 isolates including multidrug-resistant HIV-1_{MDR} (IC_{50} values of 0.2–0.6 nM) (11). AVC, despite its much greater anti-HIV-1 activity than other previously published CCR5 inhibitors including TAK-779 and SCH-C (Fig. 1), preserves RANTES and macrophage inflammatory protein-1β binding to $CCR5^+$ cells and their functions, whereas TAK-779 and SCH-C fully block the CC-chemokines/CCR5 interactions (11). AVC reportedly has an extensive and prolonged CCR5 occupancy as examined in phytohemagglutinin-activated peripheral blood mononuclear cells ($t_{1/2}$ ~ 9 h) (12) and in circulating lymphocytes in HIV-1-negative and HIV-1-positive individuals ($t_{1/2}$ of 69–152 h depending on different AVC doses) (37). In a randomized, placebo-controlled short-term monotherapy trial in patients with AIDS including those who were drug-experienced, AVC demonstrated potent antiretroviral activity and brought about significant reduction in HIV-1 viremia (by −1.7 log) in AIDS patients (38).

In the present study, we examined the profile of binding to and interactions with CCR5 of three CCR5 inhibitors, AVC, SCH-C, and TAK-779. We also conducted structural analyses of the interactions of CCR5 inhibitors with CCR5, using homology modeling, robust structure refinement, and docking. Notably, the molecular modeling analyses were combined and fine-tuned with the results of the saturation binding assay using a panel of mutant CCR5-expressing cells and [^{3}H]CCR5 inhibitors and the resultant configurations and orientations of inhibitors docked within the hydrophobic cavity of CCR5 yielded structure-activity predictions and interpretations consistent with the observed experimental data. The present approach of combining the site-directed mutagenesis-based data and molecular modeling should represent a

* This work was supported in part by the Intramural Research Program of the Center for Cancer Research, NCI, National Institutes of Health, and in part by a grant-in-aid for Scientific Research (Priority Areas) from the Ministry of Education, Culture, Sports, Science, and Technology of Japan (Monbu-Kagakusho), a Grant for Promotion of AIDS Research from the Ministry of Health, Welfare, and Labor of Japan Kosei Rohdosho H15-AIDS-001, and the Cooperative Research Project on Clinical and Epidemiological Studies of Emerging and Re-emerging Infectious Diseases (Renkei Jigyo number 78, Kumamoto University) of Monbu-Kagakusho. The costs of publication of this article were defrayed in part by the payment of page charges. This article must therefore be hereby marked "*advertisement*" in accordance with 18 U.S.C. Section 1734 solely to indicate this fact.

[1] To whom correspondence should be addressed. Tel.: 81-96-373-5156; Fax: 81-96-363-5265; E-mail: hmitsuya@helix.nih.gov.

[2] The abbreviations used are: HIV-1, human immunodeficiency virus, type 1; AVC, aplaviroc; CCR5, CC-chemokine receptor 5; MIP-1α, macrophage inflammatory protein-1α; RANTES, regulated upon activation, normal T cell expressed and secreted; CHO, Chinese hamster ovary; FCS, fetal calf serum; mAb, monoclonal antibody; TM, transmembrane; gp, glycoprotein.

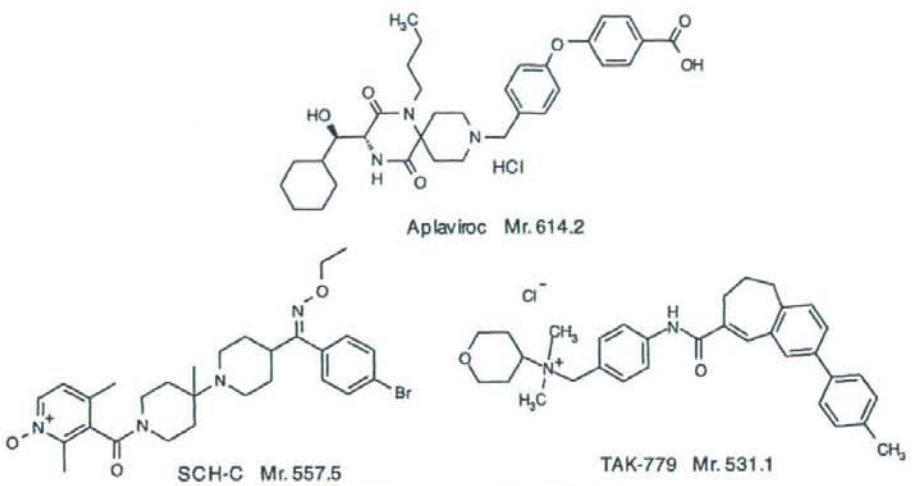

FIGURE 1. **Structures of AVC, TAK-779, and SCH-C.**

valuable strategy for gaining structural insights for membrane-bound proteins for which x-ray crystal structures are not as yet available. The present data delineating residue by residue interactions of CCR5 with CCR5 inhibitors should not only help design more potent and more HIV-1-specific CCR5 inhibitors, but also give new insights into the dynamics of CC-chemokine-CCR5 interactions and the mechanisms of CCR5 involvement in the process of cellular entry of HIV-1.

EXPERIMENTAL PROCEDURES

Reagents—A CCR5 inhibitor, AVC, was designed and synthesized as previously published (11). Two other CCR5 inhibitors, TAK-779 and SCH-351125 (SCH-C), were synthesized based on the previously published structures (13, 14) (Fig. 1). These three CCR5 inhibitors were tritiated by reductive amination with sodium triacetoxyborotritide (15), methylation with [^{3}H]methyliodide, and/or heterogeneous catalytic exchange with tritium gas (16). Two ^{125}I-labeled chemokines (macrophage inflammatory protein-1α (MIP-1α) and regulated upon activation, normal T cell expressed and secreted (RANTES)) were purchased from Amersham Biosciences and ^{125}I-labeled macrophage inflammatory protein-1β (MIP-1β) was purchased from PerkinElmer Life Sciences, Inc. Their corresponding unlabeled chemokines were purchased from PeproTech Inc. (Rocky Hill, NJ). Recombinant HIV-1_{YU2} gp120 (rgp120) and human soluble CD4 (sCD4) were purchased from Immuno Diagnostics, Inc. (Woburn, MA).

Cells and Viruses—The Chinese hamster ovary (CHO) cells overexpressing CCR5 (17) were maintained in Ham's F-12 medium (Invitrogen) supplemented with 10% fetal calf serum (FCS: JRH Biosciences, Lenaza, KS) and 50 units/ml penicillin and 50 μg/ml streptomycin in the presence of 5 μg/ml blasticidin S hydrochloride. The HeLa-CD4-LTR-β-galactosidase indicator cell line expressing human CCR5 (CCR5$^+$MAGI (multinuclear activation of galactosidase indicator) cells) (18) was a kind gift from Dr. Yosuke Maeda, Kumamoto University Graduate School of Medical and Pharmaceutical Sciences, Japan. CCR5$^+$MAGI cells were maintained in Dulbecco's modified Eagle's medium (DMEM) supplemented with 10% FCS, 200 μg/ml G418, 100 μg/ml hygromycin B, and 100 μg/ml zeomycin. The U373-MAGI cell line was obtained from the AIDS Research and Reference Reagent Program, NIAID, National Institutes of Health (Bethesda, MD). U373-MAGI cells were maintained in Dulbecco's modified Eagle's medium supplemented with 10% FCS, 200 μg/ml G418, and 100 μg/ml hygromycin B. An R5-HIV-1 strain, HIV-1_{Ba-L}, was employed for the determination of the susceptibility of mutant CCR5 ($CCR5_{MT}$)-expressing cells to the infectivity of HIV-1.

Generation of Wild-type and $CCR5_{MT}$-overexpressing Cells—A mammalian expression vector pZeoSV2 (Invitrogen) carrying the human wild-type *CCR5* ($CCR5_{WT}$) gene (pZeoSV-*CCR5*) (18) was a kind gift from Dr. Yosuke Maeda. A variety of plasmids carrying a mutant *CCR5*-encoding gene were generated using the site-directed mutagenesis technique employing the QuikChange site-directed mutagenesis kit (Stratagene, La Jolla, CA) as described by the manufacturer. Mutations introduced into the *CCR5* gene were introduced through: (i) substitution of an amino acid(s) or (ii) deletion of an amino acid(s) at selected amino acid positions of CCR5. A mutation from Gly to Arg at position 163, where the corresponding amino acid in simian CCR5 is Arg, was also introduced. This G163R substitution has been reported to reduce the binding of R5-HIV-1-gp120 to human CCR5 and the susceptibility to HIV-1 (19). All these plasmids were confirmed to contain only the desired mutation(s) by nucleotide sequencing.

CHO cells (or U373-MAGI cells) were transfected with a plasmid containing the $CCR5_{WT}$-encoding gene or a plasmid carrying a $CCR5_{MT}$-encoding gene using Lipofectamine (Invitrogen); the transfectants were magnetically sorted, following treatment with an anti-CCR5 monoclonal antibody (2D7 or 3A9; BD Pharmingen, San Diego, CA), using Dynabeads M-450 coupled to goat anti-mouse IgG (Dynal A.S., Oslo, Norway); and the cells were cloned using the limiting dilution technique.

Determination of CCR5 Expression Levels in CHO and U373-MAGI Cells—CCR5 expression levels of the various clones described above were determined using three indicators: (i) maximal amounts of [^{3}H]AVC bound to cells (B_{max}); (ii) mean florescence intensity values when stained with monoclonal antibody (mAb) 3A9; and (iii) mean florescence intensity values when stained with mAb 2D7. The antigenic epitope for 2D7 is located distant from that for 3A9 (20) and 3A9 does not compete with AVC binding to CCR5 (data not shown). The expression levels were expressed as % control ($CCR5_{WT}$-expressing cells as control), and the highest value obtained was chosen as the estimated

CCR5 expression level. There were no clones that had low values in all three indicators, thus sustaining that the current method used for the CCR5 expression levels was thought to be legitimate. CD4 and CCR5 expression levels were also determined using the quantitative fluorescence-activated cell sorting assay system (Quantum Simply Cellular Kit; Sigma) using 3A9 and 2D7 (12). For the HIV-1 susceptibility assay, U373-MAGI clones that expressed CD4 molecules ranging 10–25 × 10^4 antigen-binding sites were selected. $CCR5_{MT}$-expressing CHO cells were maintained in Ham's F-12 medium containing 10% FCS and 100 μg/ml zeomycin. $CCR5_{WT}$- and $CCR5_{MT}$-expressing U373-MAGI cells were cultured in Dulbecco's modified Eagle's medium supplemented with 10% FCS, 200 μg/ml G418, 100 μg/ml hygromycin B, and 100 μg/ml zeomycin.

Saturation Binding Assay Using ^{3}H-Labeled CCR5 Inhibitors—Saturation binding assay using ^{3}H-labeled CCR5 inhibitors was conducted and the K_D values of CCR5 inhibitors in $CCR5_{WT}$-, or $CCR5_{MT}$-expressing CHO cells were calculated as previously described (11).

Radiolabeled Inhibitor Binding/Competition Studies—$CCR5_{WT}$-expressing cells (1.5×10^5) were plated onto 48-well microculture plates, incubated for 24 h, rinsed, exposed to [^{3}H]AVC, [^{3}H]SCH-C, or [^{3}H]TAK-779 for 15 min at room temperature, subsequently exposed to various concentrations of unlabeled CCR5 inhibitors, incubated for 30 min, thoroughly washed, lysed, and the radioactivity in the lysates was counted. All experiments were performed in duplicate. The amounts of each ^{3}H-labeled CCR5 inhibitor bound to the cells are shown as mean % control values. Standard deviation values are indicated with the vertical lines. To obtain control values, the experiment was also performed without the addition of unlabeled CCR5 inhibitors.

Determination of CC-chemokine- and HIV-1 Gp120 Binding Affinity to $CCR5_{WT}$ and $CCR5_{MT}$—Binding profiles of chemokines to $CCR5_{WT}$- or $CCR5_{MT}$-expressing cells were determined using ^{125}I-labeled chemokines as previously reported (11) with minor modifications. In brief, $CCR5_{WT}$- or $CCR5_{MT}$-expressing cells (1.5×10^5) were plated onto 48-well microculture plates, incubated for 24 h, rinsed, exposed to 5 nM ^{125}I-MIP-1α, ^{125}I-MIP-1β, or ^{125}I-RANTES at room temperature for 1 h, thoroughly washed with phosphate-buffered saline, lysed with 0.5 ml of 1 N NaOH, and the radioactivity in the lysates counted. The nonspecific binding of the labeled chemokine to the cells was determined based on the radioactivity detected in the wells plated with the same number of CCR5-negative CHO (CHO-K1) cells exposed to an equal amount of ^{125}I-labeled chemokine. Determination of the binding profiles of HIV-1-rgp120 to $CCR5_{WT}$ or $CCR5_{MT}$ was also conducted. Briefly, $CCR5^+$ CHO cells were exposed to rgp120 (5 μg/ml) and sCD4 (5 μg/ml: biotinylated using EZ-link sulfo-NHS-SS-biotin (Pierce)) for 1 h at 37 °C. Cells were washed and binding of the rgp120-sCD4 complex to $CCR5^+$ CHO cells was determined using phycoerythrin-conjugated streptavidin (SA-PE: BD Pharmingen). Nonspecific binding was determined based on the mean florescence intensity of SA-PE with sCD4 but without rgp120. Because CCR5 expression levels vary among CCR5 clones, the % binding (occupancy) values for ^{125}I-chemokines and rgp120 were normalized using the following formula: % binding (occupancy) = 100 × (amount of ^{125}I-chemokine or rgp120 bound to $CCR5_{MT}$/amount of ^{125}I-chemokine or rgp120 bound to $CCR5_{WT}$) × (number of $CCR5_{WT}$/number of $CCR5_{MT}$), where numbers of $CCR5_{WT}$ and $CCR5_{MT}$ are expressed as B_{max} (cpm) or mean florescence intensity values as described above.

Determination of HIV-1 Susceptibility of $CCR5_{WT}$- and $CCR5_{MT}$-expressing Cells—The susceptibility of $CCR5_{WT}$- and $CCR5_{MT}$-expressing cells to the infection by an R5-HIV-1 strain, HIV-1_{BaL}, was determined as previously described (22). In brief, target cells ($CCR5_{WT}$- or $CCR5_{MT}$-expressing U373-MAGI cells; 10^4/well) were plated onto 96-well flat microtiter culture plates, inoculated with 100 $TCID_{50}$ of HIV-1_{BaL} on the following day, cultured for 48–72 h, stained with 400 μg/ml of 5-bromo-4-chloro-3-indolyl-β-D-galactopyranoside (X-gal), and all blue cells were counted. All experiments were performed in triplicate. For testing each $CCR5_{MT}$-expressing cell preparation, multiple (5 to 13) clones were examined. In each set of experiments, $CCR5_{WT}$-clone 1 was included and served as a standard. Percent infection in $CCR5_{WT}$- and $CCR5_{MT}$-expressing cells was determined using the following formula: % Infection = 100 × (mean blue cell number in a well)/(mean blue cell number in a well of $CCR5_{WT}$-clone 1).

Structural Modeling of the Interactions of CCR5 Inhibitors with Wild-type and Mutant CCR5 Species—An initial structural model of CCR5 was defined with homology modeling using the crystal structure of bovine rhodopsin as a template (23). This resulted in the initial placement of the helices and side chains. The CCR5-inhibitor complex structures were defined with an iterative optimization of CCR5 and inhibitor structures in the presence of each other, using software tools from Schrödinger (Schrödinger, LLC, New York), as described below. The conformational flexibility of both CCR5 and the inhibitors were taken into account. The molecular structures of AVC, SCH-C, and TAK-779, without the presence of counter-ions and solvents, were obtained by minimization using the MMFF94 force field (24). For each minimized inhibitor configuration, a set of low energy structures was generated by performing a Monte Carlo sampling of their conformations. Thus obtained structures were used as starting structures for docking calculations where their conformations were further refined.

The protonation states of CCR5 residues were assigned, and residues more than 20 Å from the active site were neutralized. In an attempt to place an inhibitor within CCR5, initially the active site was artificially enlarged by mutating Tyr^{108}, Cys^{178}, Glu^{283}, and Met^{287} to Ala. The van der Waals radii of inhibitor atoms were scaled by a factor of 0.70 to reduce steric clashes and docked into CCR5. After obtaining an initial set of CCR5-inhibitor complexes, residues 108, 178, 283, and 287 were mutated back from Ala to their original states. CCR5 atoms within 15 Å of an initially placed inhibitor were subsequently refined. It was achieved by using the rotamer library of Xiang and Honig (25) and optimizing each side chain one at a time holding all other side chains fixed. After convergence, all side chains were simultaneously energy minimized using the OPLS-AA force field (26) to remove any remaining clashes. The inhibitors were docked again and scored to estimate their relative affinity. The docked complexes with higher scores were visually examined along with the mutational data to select the best possible CCR5-inhibitor complex.

Mutated CCR5 structures were defined using the wild-type CCR5 structure and optimized using the OPLS2003 force field. Charges were taken from the force field. The minimization was carried out until the gradient was below 0.2 kJ/Å-mol. Resulting minimized structures were used as starting structures for obtaining docked complexes of mutated CCR5 with inhibitors using the protocol described above. Visualization, structural refinement, and docking were performed using Maestro 7.0, MacroModel 9.0, Prime 1.2, Glide 3.5, and IFD script from Schrödinger, LLC (New York). The extra precision mode of Glide, which has higher penalties for unfavorable and unphysical interactions, was used (27). Computations were carried out on a multiprocessor SGI Origin 3400 computer platform.

A probe radius of 1.4 Å with Connolly surfaces generated was used to define binding site cavities using the method of Exner *et al.* (28) as implemented in the MOLCAD tool in Sybyl 7.0 (Tripos, Inc., St. Louis,

TABLE 1
Binding affinity of CCR5 inhibitors to mutant CCR5s

Mutant CCR5 overexpressed on CHO cells		K_D value[a]			Gp120/sCD4 binding[b]
		Aplaviroc	SCH-C	TAK-779	
			nM		% control
Wild type		2.9 ± 1.0	16.0 ± 1.5	30.2 ± 7.6	100 ± 13.3
D11A	NH_2 terminus	3.0 ± 0.6	12.4 ± 2.0	24.5 ± 3.7	35.4 ± 4.7
Y37A	TM1	7.9 ± 0.9	>200	**98.9 ± 11.5**	35.4 ± 3.7
Y108A	TM3	**19.8 ± 4.4**[c]	11.8 ± 1.1	>200	13.2 ± 1.0
F112L	TM3	4.0 ± 2.6	30.0 ± 6.4	33.0 ± 7.2	
F112Y	TM3	6.8 ± 1.1	35.8 ± 7.6	28.5 ± 3.1	111 ± 6.9
F113A	TM3	**13.3 ± 2.3**	43.8 ± 6.3	32.7 ± 3.3	
F113Y	TM3	8.6 ± 3.4	45.3 ± 12.1	32.4 ± 3.0	
G163A	TM4-ECL2[d]	8.0 ± 4.2	25.0 ± 8.2	24.0 ± 5.9	
G163R	TM4-ECL2[d]	>200	46.3 ± 16.5	88.3 ± 22.9	34.1 ± 5.4
R168A	ECL2	**13.2 ± 3.3**	21.0 ± 8.1	43.0 ± 4.7	
K171A/E172A	ECL2	2.8 ± 0.1	34.8 ± 6.8	30.5 ± 0.7	29.6 ± 2.2
C178A	ECL2	>200	27.1 ± 4.4	34.5 ± 3.5	20.9 ± 1.0
S180A	ECL2	5.7 ± 1.2	31.8 ± 14.4	18.2 ± 3.2	
S180T	ECL2	1.5 ± 0.6	25.4 ± 6.8	41.0 ± 3.8	101 ± 15.0
S180E	ECL2	**13.9 ± 1.7**	16.5 ± 2.2	25.0 ± 3.5	51.6 ± 1.1
Y184A/S185A	ECL2	2.0 ± 0.8	21.3 ± 5.0	28.0 ± 2.5	
Y184A/S185A/Q186A/Y187A	ECL2	2.0 ± 0.6	14.9 ± 0.6	32.3 ± 5.8	
Q186A/Y187A	ECL2	2.8 ± 0.5	14.7 ± 8.8	35.2 ± 5.8	
Q188A	ECL2	6.6 ± 1.4	23.8 ± 1.5	37.9 ± 2.5	
WKNF190del	ECL2-TM5	>200	**49.2 ± 1.7**	80.1 ± 16.7	
K191A	ECL2-TM5	>200	26.5 ± 7.1	35.0 ± 3.8	45.7 ± 0.6
K191R	ECL2-TM5	**9.0 ± 5.6**	34.1 ± 19.1	47.1 ± 8.8	
K191N	ECL2-TM5	**14.2 ± 1.1**	35.8 ± 9.2	35.1 ± 9.3	
K197A	TM5	**9.2 ± 4.3**	16.8 ± 2.9	14.7 ± 1.1	
I198A	TM5	**24.6 ± 4.8**	**52.4 ± 3.0**	54.9 ± 6.9	51.7 ± 3.0
Y251A	TM6	**36.5 ± 9.5**	21.5 ± 8.6	43.0 ± 4.5	14.5 ± 0.7
E283A	TM7	>200	>200	>200	4.3 ± 0.6
M287A	TM7	6.8 ± 2.3	28.0 ± 9.1	39.8 ± 7.5	104 ± 3.9
M287E	TM7	**14.8 ± 1.7**	32.2 ± 4.2	53.1 ± 3.7	22.0 ± 0.8

[a] K_D values were determined using saturation binding assays ("Experimental Procedures").
[b] Gp120/sCD4 binding affinity to $CCR5_{MT}$ is shown by % control (see "Experimental Procedures" for reference); the data are also shown in Fig. 8*A*.
[c] K_D values more than 3-fold compared to that with $CCR5_{WT}$ are shown in bold. All K_D values were determined on multiple occasions (twice to 6 times). Considering the standard deviation for the wild type and other mutations, a 3-fold difference was seen to be statistically significant.
[d] ECL, extracellular loop.

MO). Lipophilic potential was mapped onto the cavities using parameters from Viswanadhan *et al.* (29).

RESULTS

Site-directed Mutagenesis of CCR5 and Binding Affinity of CCR5 Inhibitors—We have previously reported (11) that AVC competitively blocked the binding of a monoclonal antibody, 45531, which is known to be specific against the C-terminal half (or domain B) of the second extracellular loop (ECL2B) of CCR5 (21), whereas AVC failed to block or only partially blocked the binding of two other monoclonal antibodies, 2D7 and 45523, specific for CCR5 but not for its ECL2B. When we examined three additional monoclonal antibodies, 3A9 and 45502 (both specific for NH_2 terminus) and 45549 (multidomain reactive) (20, 21), none of these antibodies were replaced by AVC (data not shown). These data suggest that the potent inhibitory activity of AVC against R5 HIV-1 infection stems from its binding to ECL2B and/or its vicinity with high affinity.

In an attempt to delineate the CCR5 binding profile of the three CCR5 inhibitors, we generated a variety of CCR5 mutant-overexpressing ($CCR5_{MT}$) CHO cells and determined the K_D values of each inhibitor to mutant CCR5 species using the saturation binding assay with tritiated inhibitors. When we determined the K_D value of AVC with respect to a CCR5 mutant carrying an Asp to Ala substitution at position 11 of the amino terminus domain ($CCR5_{D11A}$), the value was 3.0 nM, virtually identical to the K_D value with wild-type CCR5 ($CCR5_{WT}$; Table 1), indicating that the D11A substitution did not affect the binding of AVC to CCR5. The K_D value of AVC with respect to $CCR5_{Y37A}$ was moderately greater with 7.9 nM (2.7-fold compared with the K_D value with regard to $CCR5_{WT}$). On the other hand, those of TAK-779 and SCH-C to $CCR5_{Y37A}$ were 98.9 nM (3.3-fold compared with the K_D with regard to $CCR5_{WT}$) and >200 nM (>12.5-fold), respectively, in agreement with the previous reports in which both TAK-779 and SCH-C apparently failed to bind, probably explaining that these inhibitors failed to block HIV-1 infection of $CCR5_{Y37A}$-expressing cells (30, 31). These data suggest that the binding of TAK-779 and SCH-C to $CCR5_{WT}$ is more dependent on interactions with Tyr37 than that of AVC. We also generated a series of CCR5-overexpressing CHO cells carrying a mutation(s) at a selected amino acid position(s). As shown in Table 1, the mutations that substantially (more than 3-fold compared with AVC binding to $CCR5_{WT}$) affected the K_D values of AVC were as follows: Y108A and F113A in the third transmembrane domain (TM3) of CCR5; R168A and S180E in ECL2; K191R and K191N of the interface of ECL2B and TM5; K197A and I198A of TM5; Y251A of TM6; and M287E of TM7. The mutations that greatly diminished the binding of AVC (values of >200 nM) to CCR5 were as follows: G163R, C178A, WKNF190del, K191A, and E283A. It is worthwhile to interject that Lys^{191} in ECL2 is reported to be critical for the binding of RANTES, MIP-1α, and MIP-1β to CCR5 (32, 33), whereas Cys^{178} is presumed to form a disulfide bond with Cys^{101} of ECL1 and to be critical for the conformation of CCR5 (34). Mutations that substantially affected the binding of TAK-779 and SCH-C to CCR5 were as follows: Y37A, Y108A, and E283A for TAK-779; and Y37A, WKNF190del, I198A, and E283A for SCH-C. It is noteworthy that the number of mutations that affected the binding of AVC was notably greater than those of TAK-779 and SCH-C. Thus, the CCR5 binding modes of AVC, TAK-779, and SCH-C apparently share some similar features but also have some distinct differences.